THE PERFORMANCE OF A REACTOR USING PHOTOCATALYSIS TO DEGRADE A MIXTURE OF ORGANIC CONTAMINANTS IN AQUEOUS SOLUTION

By

FREDERICK ROLAND HOLMES

A THESIS PRESENTED TO THE GRADUATE SCHOOL
OF THE UNIVERSITY OF FLORIDA IN PARTIAL FULFILLMENT
OF THE REQUIREMENTS FOR THE DEGREE OF
MASTER OF ENGINEERING

UNIVERSITY OF FLORIDA

2003

This document is dedicated to my wife April and all of the people who have helped me along the way.

ACKNOWLEDGMENTS

I would like to begin by thanking my professor and advisor Dr. Paul A. Chadik. His help in this research and my other education has been invaluable. I would also like to extend my appreciation to the other members of my committee, Dr. David Mazyck and Dr. Chang-Yu Wu.

I would like to thank the members of the Photocatalysis Seminar, especially Dr. Powers, for their knowledge and suggestions on this research. I am also thankful for all of the guidance and time Dr. Booth provided to this research in performing the analyses.

Additionally, I would like to thank NASA for providing the funding and support for this research. I thank Jack Drwiega for putting together the reactor support and I would like to thank Danielle Londereé for providing the formula used in creation of the silica/titania photocatalyst.

Lastly, I would like to thank my family, Stanley, Patricia, Vincent, and Shannon Holmes. Most importantly, I would like to thank God and my wife April. Without either of them I could not accomplish the things that I have.

TABLE OF CONTENTS

page

LIST OF TABLES

LIST OF FIGURES

Abstract of Thesis Presented to the Graduate School
of the University of Florida in Partial Fulfillment of the
Requirements for the Degree of Master of Engineering

THE PERFORMANCE OF A REACTOR USING PHOTOCATALYSIS TO DEGRADE A MIXTURE OF ORGANIC CONTAMINANTS IN AQUEOUS SOLUTION

By

Frederick Roland Holmes

August 2003

Chair: Dr. Paul A. Chadik
Major Department: Environmental Engineering Sciences

A study was performed to investigate the use of an annular reactor filled with photocatalyst pellets (silica gel support doped with Degussa P25 titanium dioxide) arranged in a packed-bed-style to oxidize selected organic chemicals in aqueous solution. The annular reactor had a volume of 436 mL with 327 mL of that being interparticle space. The reactor was configured to a system setup which included a source tank, the reactor, a PTFE (polytetrafluoroethylene) tubing pump head with modular speed drive, a dampener for controlling flow, 2 sampling ports, and a test stand to hold the reactor with slots for four 8-watt UV lamps.

Eight target analytes (acetone, butyl alcohol, carbon disulfide, chlorobenzene, ethyl acetate, indole, methyl methacrylate, and toluene) were tested for degradability in a mixed solution within the reactor system. Volatile losses were assessed as many of these chemicals are classified as VOCs.

The photocatalyst pellets were found to be capable of adsorbing target analytes when exposed to solution containing the target analytes. When exposed to solution devoid of the target analytes, however, desorption of the analytes from the silica-titania pellets occurred.

Optimization was investigated with respect to UV radiation intensity and empty bed contact time (EBCT). One UV lamp resulted in the same level of degradation of contaminant as three UV lamps. An increased EBCT was found to increase the photocatalytic degradation observed in the reactor.

All 8 of the target analytes were shown capable of complete oxidation using the reactor system. Degradation rate constants (k values) of .019 min^{-1}, .065 min^{-1}, .057 min^{-1}, .059 min^{-1}, and .128 min^{-1} were found for acetone, chlorobenzene, ethyl acetate, methyl methacrylate, and toluene respectively. These rate constants are comparable to those experienced by other researchers working with a slurry of TiO_2.

CHAPTER 1
INTRODUCTION

The goal of the research discussed in this thesis is to provide a finishing process for treating the wastewater produced by NASA in their Advanced Life Support System (ALS). NASA is in the planning stages of a manned space trip to Mars (Lane and Behrend, 1999). The ALS is to provide the support system allowing astronauts to travel the estimated 266 days to complete the mission. Fresh water that meets the requirements set forth in the Requirements Definition and Design Consideration (Lange and Lin, 1998) is an important part of the ALS. These requirements are displayed in Table 13 (Appendix A). High-energy costs are incurred to move mass in NASA space missions. As a result, NASA desires to minimize the amount of mass required for space transport. This means that in addition to treating the wastewater, the finishing process must do so while minimizing space and energy requirements.

Wastewater will be collected through two different sources in the space module. One source of wastewater is from the crew in the module. Shower water, wash water, urine, and wastewater from the solid waste processor are among the contributors to the wastewater stream. Machinery within the ALS will be the second source of wastewater. Condensate on the walls, panels, and instruments will be collected for treatment. A list of all organic contaminants expected in the ALS wastewater is found in NASA documentation, provided in Table 14 (Appendix A). The rate that this water is expected to be produced is 28 L/person/day based on an assumed number of six astronauts.

Collected wastewater from the ALS will be treated through a series of treatment processes. Those processes include biological removal, ion exchange, reverse osmosis, and chemical disinfection. These processes remove many water contaminants; however, there remain some organic chemicals and microbial constituents in the water that are not expected to be removable by the aforementioned treatment processes. Of those remaining chemicals, the 8 shown in Table 1 were chosen as target analytes for this research. This thesis focuses on a finishing process to remove these chemicals.

Table 1. Target Analytes

Acetone
Butyl Alcohol
Carbon Disulfide
Chlorobenzene
Ethyl Acetate
Indole
Methyl Methacrylate
Toluene

The process chosen for study as a potential NASA finishing process is photocatalytic oxidation. Photocatalysis was chosen as a viable option due to its potentially small mass, space, and energy requirement. In addition, photocatalysis has been shown to be effective for the removal of organic compounds, inorganic compounds, and microbes. This thesis will only consider the removal of the organic chemicals shown in Table 1. Included in the compounds that have proven removable are three among the target contaminants for this research, chlorobenzene (Rohrbacher, 2001), acetone (Hingorani et al., 2000), and toluene (Vijayaraghavan, 2000; Luo and Ollis, 1996).

This research was performed in a 436 mL flow-through annular reactor designed for the purpose of maximizing exposure of the photocatalyst to the ultraviolet (UV) light. A previously designed silica-titania composite (Londeree, 2002) was used as the

photocatalyst in the reactor. The photocatalyst was formed into a pellet of approximately 3 mm diameter. These pellets were then packed within the annular reactor. Solutions containing the target analytes were subjected to photocatalytic oxidation treatment within the reactor, and the product waters were analyzed using gas chromatography / mass spectrometry (GC/MS) and gas chromatography / flame ionization detection (GF/FID) to asses the efficiency of the treatment process.

The hypothesis for this research was that an annular reactor, filled with a titania/silica composite, and arranged in a packed bed formation could be used to photocatalytically oxidize the eight target analytes listed in Table 1. Several objectives were set forth in this research to accomplish the proving of this hypothesis.

- Demonstrate the reactor's ability to degrade the 8 target analytes (acetone, butyl alcohol, carbon disulfide, chlorobenzene, ethyl acetate, indole, methyl methacrylate, and toluene).
- Determine the reactor's optimal degradation performance with respect to UV intensity and flow rate (contact time).
- Quantify reaction rate constants for removal of the organic chemicals.
- Assess the reactor's effluent conductivity, dissolved oxygen concentration, pH, and temperature.

CHAPTER 2
LITERATURE REVIEW

Photolysis and Photocatalysis

The degradation of both organic and inorganic constituents with light has been well established. The words degradation and photocatalytic oxidation used in this thesis will always refer to the disappearance of the initial compound or transformation of that compound into another. The words do not mean that the contaminant has been completely oxidized or entirely removed. Degradation has been achieved using two main methods important to the current research, photolysis and photocatalysis.

Photolysis is a process that involves the use of light to degrade molecular compounds toward their base constituents, often carbon dioxide and water. During photolysis a direct photochemical transformation takes place where energy from light attacks the bonds within a molecular compound, thereby degrading the compound. Unfortunately, not all compounds can be degraded in this manner. Specifically, chlorobenzene cannot be degraded photolytically (Nishida and Ohgaki, 1994). For this reason, photocatalysis becomes necessary.

Photocatalytic oxidation uses light energy to react with a molecule leading to the formation of radicals in the solution. Several different molecules have been shown capable of promoting photocatalysis, from methylene blue (Cooper and Goswami, 1999), to ZnO (Sakthivel et al. 2002), to TiO_2 (Goswami et al., 1997). The radicals can be formed from the molecule itself or from constituents in the solution containing the molecule. These radicals are then capable of oxidizing or reducing and thereby

destroying the target contaminants. There are three known highly reactive intermediates formed by the process of photocatalysis, $^1O_2$ (oxygen singlets), OH· (hydroxyl radicals), and H_2O_2 (hydrogen peroxide). Research suggests that the OH· is the prominent player in photocatalysis (Turchi and Ollis, 1990). The hydroxyl radical's ability to degrade contaminants comes from its high level of oxidation power, which is more than twice as strong as chlorine (Goswami and Blake, 1996). The hydroxyl radical breaks down chemicals through a series of steps. The exact steps by which the degradation process takes place are not known, but the generally accepted hypothesis is that hydrogen atoms are removed and oxygen atoms are added. It is also known that the process is preferential to attacking double bonds as opposed to single (Emanuel, 1984).

Heterogeneous photocatalysis has been used to enhance the general process of photocatalysis. Heterogeneous photocatalysis uses a metal or dye, which is not the target of degradation, to absorb the electromagnetic energy and create the hydroxyl radicals. Titanium dioxide (TiO_2) has been the most popular choice as a catalyst for use in heterogeneous photocatalysis, because TiO_2 is inert under most conditions and therefore unlikely to react directly with the target compounds. TiO_2 has been shown by many researchers to be very effective as a photocatalyst (Chen et al., 1995; D'Oliveira et al., 1990). UV radiation at approximately 388 nm strikes the TiO_2 particle exciting an electron from the ground state to an excited state (388 nm is the chosen wavelength of light because it provides the necessary energy to excite the electron). At this point an

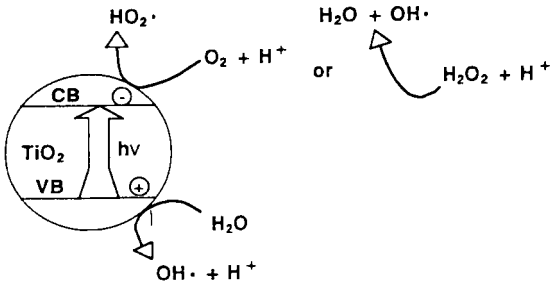

(Blake et al., 1991)

Figure 1: Figure demonstrating the elevation of an electron from one energy state to another due to UV radiation. Several possible electron donors (O_2, H_2O_2) and H_2O) are then shown adding their electron to the hole and producing their products.

electron acceptor, typically oxygen, accepts the excited electron leaving an electron hole on the surface of the TiO_2 (Turchi and Ollis, 1990). This hole is then available to accept electrons from OH^- ions, oxygen, or water to create the hydroxyl radicals. Those radicals then oxidize the pollutants in the water. The following equations describe the process of using OH^- as the precursor for the radicals and then the effects of the radical formation (Blake et al., 1991).

$$OH^- + TiO_2 + hv \rightarrow TiO_2^- + OH\cdot \quad \text{(Eq.1)}$$

$$TiO_2^- + O_2 + H^+ \rightarrow TiO_2 + HO_2\cdot \quad \text{(Eq.2)}$$

$$2HO_2\cdot \rightarrow H_2O_2 + O_2 \quad \text{(Eq.3)}$$

$$TiO_2^- + H_2O_2 + H^+ \rightarrow TiO_2 + H_2O + OH\cdot \quad \text{(Eq.4)}$$

$$\text{Pollutant} + OH\cdot \rightarrow POH\cdot \quad \text{(Eq.5)}$$

$$POH\cdot + (O_2, H_2O_2, OH\cdot) \rightarrow nCO_2 + mH_2O \quad \text{(Eq.6)}$$

Factors Affecting Photocatalysis

As previously discussed, there are several steps required in carrying out the process of photocatalytic oxidation. Any of those steps have the potential to limit the rate of

pollutant degradation. The following sections will discuss factors that play a part in enhancing or retarding the photocatalytic process.

Reactor Type

TiO_2 has been studied through two different modes of contact with contaminated waste streams. One method is to introduce slurry of TiO_2 to the wastewater. The other method involves fixing the TiO_2 to a surface, often a filter or the outside of a tube and then moving the water over the surface of the TiO_2. Both methods have their limitations. When using a TiO_2 slurry degradation of the target pollutants is often highly efficient; however, the complication comes from the inability to effectively remove the TiO_2 from the effluent water. The average size of Degussa P25 TiO_2 (the brand used in this research) is only 21 nm in diameter, and therefore expensive filtration systems would be required to remove the TiO_2 rendering the entire process not viable for space missions. Fixing the TiO_2 to a surface solves the issue of TiO_2 in the effluent but yields other disadvantages. Scouring of TiO_2 from the fixed surfaces has been observed (Butterfield et al., 1997). The more pressing concern is that the short life of the $OH\cdot$ can lead to situations where the contaminant may not come into contact with the TiO_2 surface and thus never be degraded. "The convenience of catalyst immobilization is bought at the price of diffusion distance from pollutant to catalyst surface" (Ollis et al., 1991). This led to the concept of immobilization of the TiO_2 on particles creating slurry that would later be easily removable due to its larger size (for this research approximately 3 mm in diameter).

pH

One of the most problematic factors affecting the use of photocatalysis as a viable means of water treatment is pH. Understanding the effect of pH is difficult due to the

mixed results obtained during experimentation. The effect of pH on the removal of distillery effluent (Zaidi and Goswami, 1995) and 3-Chlorophenol (D'Oliveira et al., 1990) was found to be minimal, while the effect of pH on the removal of toluene was found to be significant (Vijayaraghavan, 2000). Highly acidic solutions (pH ≅ 3) have been found to assist in the degradation of some molecules such as chlorobenzene that were found to have an optimum pH of 3.5 (Kawaguchi, Furuya, 1990). A high pH (pH ≅ 10) has also been found to help in the oxidation of ammonia and trace organics (Bonsen et al., 1997; Chen et al., 1995). Low pH preference has been explained as the ability of the H_2O_2 to make more OH· (Chen et al., 1995). A high pH has been credited with providing enough of the necessary hydroxyl ions for making the hydroxyl radicals (D'Oliveira et al., 1990; Chen et al., 1995). The research indicates pH will be an important factor to assess in the analysis of photocatalysis as an effective means of treatment for the ALS.

Dissolved Oxygen (DO)

Dissolved oxygen (DO) in sufficient amounts has been found by multiple researchers to be a necessity to the photocatalytic process. Hand et al. (1995) found that below 2.0 mg/L the rate of degradation for disinfection byproducts was significantly decreased. Vijayaraghavan (2000) found that when sodium sulfite was used to remove oxygen from water that was then contaminated with toluene, the rate of toluene degradation was significantly decreased. Other researchers have made statements about the importance of DO in the photocatalytic oxidation process (Zaidi and Goswami, 1995; Ollis et al., 1991). "Several researchers have observed that oxygen adsorbed on the titanium dioxide surface prevents the recombination of hole/electron pairs by trapping

electrons and therefore, plays an important role in semiconductor mediated reactions" (Vidal, 1998). It does stand to reason that a replacement electron acceptor could be found, such as H_2O_2 (Ollis et al., 1991). However, it is likely that oxygen will prove to be the cheapest and safest electron acceptor for use in the space missions, and for this reason oxygen will be the electron acceptor used in this research.

Intermediates

Formation of oxidation intermediates in the photocatalytic reaction is a concern in water treatment because some intermediates have the potential to be more toxic than the original contaminants (Torimoto et al., 1996). Intermediates also occupy sites on the surface of the TiO_2 where the photocatalytic reactions with target compounds are meant to occur (Chen et al., 1995). Several intermediates have been detected in a variety of degradation processes. Catechols, hydroquinones, biphenyls, formaldehyde, and glyoxal, are a few of the intermediates that have been detected during the photocatalytic degradation of hydrocarbons and aromatics (Kawaguchi and Furuya, 1990; Denisov, 1977). One series of experiments claims that the use of TiO_2 on the surface of activated carbon suppressed the amount of intermediates in the solution by trapping the intermediates until they were fully degraded by photocatalysis (Torimoto et al., 1996).

Bicarbonate Alkalinity

Alkalinity in the water has been shown to significantly decrease the rate of photocatalytic oxidation in several cases. One researcher observed as much as a 67% decrease in the photocatalytic degradation rate of chlorobenzene when 500 mg/L of HCO_3^- was added to the water (Blake et al., 1991). Bekbölet (1996) observed a significant decrease in the degradation of humic acids. He attributed the decreased rate to bicarbonate ions scavenging the hydroxyl radicals that are necessary for photocatalysis.

Equation 7 describes the reaction whereby bicarbonate ions and hydroxyl radicals react to form water and the significantly less powerful oxidant, the carbonate radical.

$$HCO_3^- + OH\cdot \rightarrow \cdot CO_3^- + H_2O \qquad \text{(Eq.7)}$$

Light Intensity

Illumination of the photocatalyst at an appropriate intensity is essential to the photocatalysis process. Some observations have suggested that photocatalysis may even be impossible for water with high turbidity levels capable of blocking out light (Anheden et al., 1996). Most research appears to agree that there is a balance to be found with increasing or decreasing the light intensity. One study suggests that a decrease in UV intensity decreased the energy consumption and yet increasing UV intensity decreased the efficiency of energy use (Klausner and Goswami, 1993). Light intensity application is a balance between capital cost and operating costs. A higher light intensity will increase the rate of the reaction meaning a smaller reactor size will be required leading to a lower capital cost and a higher operating cost. A decrease in light intensity will decrease the operating costs, but increase the size of the reactor required to achieve a specified level of photodegradation. There is a limit at which an increase in UV intensity no longer increases the photocatalysis rate as some other step in photocatalysis will become rate limiting. Ollis et al. (1991) reported that at low intensities the degradation rate is linearly dependent upon intensity. In some (not quantitatively defined) intermediate range there is a square root dependence on intensity (I) where the rate varies as $I^{0.5}$. Finally there comes a point at high UV intensities where the rate no longer has any dependence on UV radiation. UV intensity is also based on the refraction of light caused by the TiO_2 itself and the contaminants within the wastewater to be treated. This

is due to the scattering of the light photons required for exciting the TiO_2's electrons (Chen et al., 1995; D'Oliveira et al., 1990).

Temperature

The effects of temperature on photocatalysis are mixed in the research literature. One study found a linear increase in the degradation rate of toluene with increasing temperature up to 90 °C (Vijayaraghavan, 2000). It would appear that with regards to diffusion of $OH\cdot$ from the surface of the TiO_2 to the pollutant a higher temperature would increase the photocatalytic reaction rate. Higher temperatures may have a negative effect, however, on the concentration of dissolved oxygen in the solution. Dissolved oxygen levels below a certain point may allow for electron-hole recombination at the surface of the TiO_2. Electron-hole recombination is dominant unless there is an electron acceptor such as oxygen available to absorb the excited electron.

Other Factors

There are many other factors that can affect photocatalysis. Common acids and anions have been shown to affect photocatalysis. The effect of HCO_3^- has already been mentioned for its effects as alkalinity. The rate of mineralization of targeted contaminants has also been shown to decrease in the presence of the following acids: HCl, H_3PO_4, H_2SO_4, HNO_3, and perchloric acid in the order shown at the top of page 18 (Ollis et al., 1991).

$$HCl > H_3PO_4 > H_2SO_4 > HNO_3 > \text{perchloric acid}$$

Inorganic substances and salts have also been found to decrease the reaction rates (Block et al., 1997; Vidal, 1998), because they take up sites on the TiO_2 preventing the OH^- from reacting with holes on the TiO_2 surface. Additionally, some of these substances have the possibility of reacting with the hydroxyl radical after it forms.

Enhancements to the Photocatalyst and Solution

Several different methods may be used to enhance the process of photocatalysis. Possible additives to the photocatalyst are platinum, tungsten, palladium, peroxydisulfate, silver, and ferrioxalate (Goswami, 1995; Goswami, 1999; Ollis et al., 1991; Crittenden et al., 1997). The addition of hydrogen peroxide to the contaminated solution is another enhancement method that has been intensely studied. Varying the pollutant concentration has also been found to affect the photocatalytic rate (Anheden et al., 1996). Various supports for the photocatalyst have also been tried. The advantages and disadvantages to each of these enhancement possibilities are discussed in the following sections.

H_2O_2

Hydrogen peroxide is a potential additive to the photocatalytic process that has been studied in depth. Addition of H_2O_2 has produced widely different results under varying circumstances. Hydrogen peroxide has been shown to increase the rate of mineralization of target compounds eleven fold (Lichtin et al., 1992). However, it has also been shown to decrease the rate of photocatalysis (Bekbölet and Baleioglu, 1996). This wide variance is not surprising based on Equations 8-10 (Bekbölet and Baleioglu, 1996).

$$e^- + H_2O_2 + H^+ \rightarrow H_2O + OH\cdot \qquad \text{(Eq. 8)}$$

$$H_2O_2 + OH\cdot \rightarrow H_2O + HO_2\cdot \qquad \text{(Eq.9)}$$

$$HO_2\cdot + OH\cdot \rightarrow H_2O + O_2 \qquad \text{(Eq.10)}$$

Equation 8 shows hydrogen peroxide as an electron acceptor similar to that of oxygen. Research has found that the use of H_2O_2 can help make up for a lack of oxygen (Ollis et al., 1991). Equation 8 also shows the production of a hydroxyl radical, which is also a benefit to the photocatalytic process. Equations 9 and 10 demonstrate the problem with

hydrogen peroxide; it will consume hydroxyl radicals meant for attacking the target pollutants. One researcher (Bekbölet, 1996) said that, "it could be seen that the degradation of humic acid first increased when hydrogen peroxide increased and reached a maximum beyond which they appeared to decline at high H_2O_2 doses."

TiO_2 Supports

In an attempt to overcome the issues surrounding the method of contact between the solution and the photocatalyst, many supports have been tried. Silica, activated carbon, glass beads, and filters represent the bulk of the research into support structures for TiO_2. Each support has its particular benefits and detriments. For the NASA research, a silica gel support was chosen due to its transparency to UV radiation and possible adsorption capability for the contaminants.

Activated carbon

Activated carbon offers the advantage of added surface area to adsorb pollutants and intermediates, holding them near the site of hydroxyl radical formation. Activated carbon is, however, opaque and so will have a negative impact on the amount of UV energy reaching the TiO_2 particles. For this reason activated carbon was not used as a support structure in this research.

Glass beads and filters

Both glass beads and filters have been studied in past research as possible support structures for TiO_2 (Ollis and Al-Ekabi, 1993). Although both have demonstrated minor efficiency in degrading specific target compounds, there are concerns with both methods. One concern is that the TiO_2 may be scoured off of either surface (Bideau et al., 1995). A second problem is that adsorption of contaminants and intermediates to these surfaces

is not probable. For these reasons neither of these supports was chosen for use in this research.

Silica gel

The use of SiO_2 as a support offers several benefits. Pore structure, surface area, and hydroxyl groups that encourage the adsorption of pollutants to its surface (Yu and Wang, 2000; Liu, Cheng, 1995; Gao and Wachs, 1999) are among the advantages to using a silica gel matrix as the support structure for the TiO_2. Importantly, it offers these benefits without compromising the ability of the light energy to strike the TiO_2 particles (Matsuda et al., 2000).

Having noted the benefits pointed out in the literature it is important to recognize that there is research that indicates disadvantages to using silica gel as a photocatalyst support. Matthews (1998) performed an experiment using a reactor similar to the one built for this current NASA research. A silica gel matrix was used as an adsorbent support for TiO_2, and this system achieved excellent degradation of the target compounds. However, in a later article (Ollis and Al-Ekabi, 1993), Matthews reported that the degradation of the initial compounds was promising, but the byproduct formation rendered the process not viable for treatment. Matthews went on to state the reason as being due to the byproducts becoming trapped in pores of the silica gel that do not receive contact from hydroxyl radicals produced near other pores on the silica gel surface. The main difference between the research of Matthews and that being reported in this thesis is the concentration of TiO_2 in the silica gel. The pellets created by Matthews (.15 g TiO_2 per 80 g SiO_2) contained two orders of magnitude less titanium dioxide than that of the ones designed by Londeree (2002) for this research. Presumably, this increased ratio of TiO_2 to SiO_2 will allow for photocatalysis over the entire surface of

the silica gel preventing intermediates from escaping into solution without exposure to photocatalysis.

SiO_2/TiO_2

The process of creating a TiO_2/SiO_2 catalyst can be carried out in different ways and no one way has currently been proven to be the superior method. The types of TiO_2/SiO_2 catalysts are classified as two general types. There are the structures where the TiO_2 is contained within the pores and within the gel as TiO_2 (Londeree, 2002). In this particular case there is no chemical combination of the SiO_2 with the TiO_2. The SiO_2 gel physically contains the TiO_2 particles. In the second case there are actual chemical bonds formed between the Ti element and the Si element. The presence of Si-O-Si bonds, Ti-O-Ti bonds, and Si-O-Ti bonds have been studied and confirmed (Nawrocki, 1997; Liu and Cheng, 1995; Matsuda et al., 2000; Gao and Wachs, 1999). Currently, the process being used in the NASA research is a method of doping the SiO_2 sol-gel while it is being created with solid TiO_2 particles. This would be counted under the first classification of catalyst described where the particles are physically trapped within the silica gel, but not chemically bonded.

Sol-gel structure

The structure of the sol-gel is very important to the benefits received from it. The hydroxyl concentrations on the SiO_2/TiO_2 surface contribute to the ability of the catalyst to adsorb pollutants. Adsorption of the pollutants directly to the catalyst decreases the distance the hydroxyl radical has to travel in order to degrade the pollutant. This is important considering the short life of the hydroxyl radical in solution. Nawrocki (1997) gave these 10 facts about the surface structure of the silica gel.

- The hydroxyl concentration on the surface of the SiO_2 (silanol groups) is accepted to be approximately 8.0 ± 1.0 μmol/m^2.
- These hydroxyl sites come in three different types, isolated, geminal, and vicinal.
- The isolated sites involve a hydroxide ion attached to a silicon atom on the outer edge of the gel.
- Geminal sites are characterized by two hydroxide ions attached to the gel at the same point.
- Vicinal sites have two hydroxyl groups joined to the gel at two different sites, but a hydrogen group from one is also bonded to the oxygen group from the other.
- Isolated and geminal silanol groups are the most effective at adsorbing pollutants, particularly organics. The difficulty lies in obtaining the isolated hydroxyl groups on the surface of the gel.
- Rehydroxylation and dehydroxylation are the two methods for controlling the type of silanol groups.
- Rehydroxylation is achieved through exposing the gel to water. As the silica gel is rehydroxylated the number of vicinal groups increases. This means less isolated and geminal groups are available for the attachment of pollutants.
- The gel is treated at high temperatures to remove the silanol groups during dehydroxylation. Heating the gel initially removes water that is attached to the silanols. It will then remove the bonded silanol groups leading to a slight increase in the number of isolated and geminal sites. Lastly, all of the silanol groups are removed, leaving a surface of just oxygen.
- Achieving a balance between rehydroxylation and dehydroxylation would create the ideal gel, as it would provide for the maximum possible number of isolated and geminal sites on the gel surface. This is important since these sites are the ones capable of enhancing adsorption. Unfortunately, without the addition of organics to the surface of a silica gel during gel formation, it is not possible to maintain a balance in solution. This is due to the rapid rehydroxylation that occurs in aqueous solution.

Degradable Compounds

The ability for TiO_2 to degrade many different compounds with or without the help of SiO_2 and other additives is an area that has been the focus of many researchers. Table 2 (Blake, 1999) lists a number of compounds that have been researched and shown

capable of being mineralized; however there is a lack of studies reported on TiO_2 photocatalysis in solutions involving a mixture of chemicals. In this NASA project an aqueous mixture of 8 chemicals will be investigated. It's expected that one hindrance to the photocatalytic reaction rate caused by the use of a mixture will result from the availability of sites on the TiO_2 particles. This is the same problem experienced in a solution with just one pollutant. The possibility also exists for an increase in the obstruction of light from the photocatalyst. One important and unpredictable problem lies with the production of intermediates. Because there are so many intermediate combinations possible with the compounds being tested. There are a multitude of reactions and interactions that could then occur between those formed intermediates.

Table 2: Researched Compounds

Degradable Compounds	Researcher
Bacteria and Viruses	(Goswami et al., 1997)
B-TEX	(Srinivasan et al., 1997)
Chlorinated Hydrocarbons	(Crittenden et al., 1997)
Organics	(Matthews, 1987)
Mono- and Di- Chlorobenzene	(Kawaguchi and Furuya, 1990)

Non-Degradable Compounds	Researcher
Carbon Tetrachloride	(Ollis, 1983)

Reaction Kinetics

The Langmuir-Hinshelwood (LH) equation has been shown by Klausner (1994) to appropriately model the kinetic reaction rates of photocatalysis.

$$dC/dt = -k_1KC/(1+KC) \qquad \text{(Eq.11)}$$

where C is the bulk concentration of contaminant in the solution, k_1 is the reaction rate constant and K represents the equilibrium adsorption constant for a particular contaminant to the photocatalyst (Turchi, Ollis, 1989).

It is important to note that the use of the LH equation to describe photocatalytic kinetics makes an assumption that adsorption of the contaminant to the TiO_2 surface is the rate limiting step. At low bulk concentration values, the LH equation becomes equivalent to a first order reaction equation, as the TiO_2 will not be saturated at the surface. Since all of the concentrations used in this research will be at or below 300 μg/L, the first order reaction will likely be applicable; however this also relies on low K values. Figure 2 depicts a Langmuir-Hinshelwood curve. From this curve, it can be seen that the lower concentrations appear to have a first order reaction rate while the higher concentrations move away from the first order model.

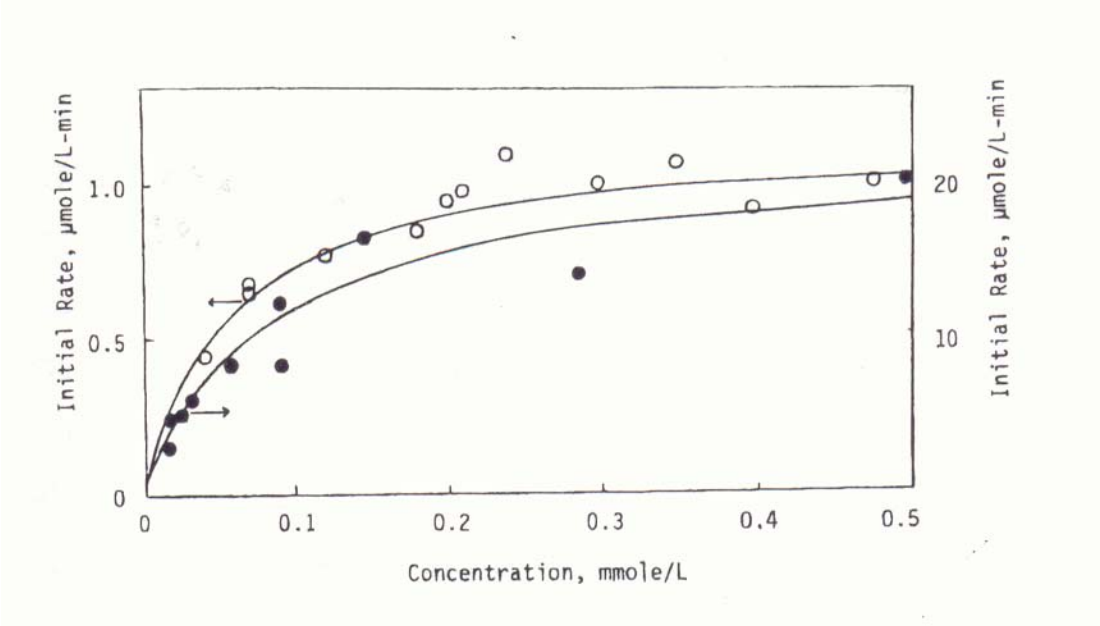

(Davis and Hao, 1991)

Figure 2. A curve showing a series of experiments that were modeled using the Langmuir-Hinshelwood equation.

Summary

Photocatalysis is a complex process of interactions between the photocatalyst, the reactants, and light. Literature comes to no valid consensus on some of the parameters'

effects on the process. pH data provides mixed results, temperature is inconclusive, and the use of hydrogen peroxide as an aid has been proven and disproved. However, other parameters have been shown to have definitive effects. UV radiation intensity has been shown to directly affect photocatalytic oxidation rates to a point. It has also been shown that the rate of flow through a reactor using fixed TiO_2 can have an impact on the amount of degradation due to the short life span of $OH\cdot$. This thesis investigates the effect some of these parameters have on this specific reactor using the photocatalysis process.

CHAPTER 3
METHODS

Assessing of the reactor's capabilities for degrading NASA's 8 target analytes required several steps. First, the photocatalyst was created. This was done in accordance with a predetermined method (Londeree, 2002). Secondly, a suitable reactor was designed for the process. UV transmission and the ability for the reactor to be included into a system that would allow for testing of the reactor were important factors considered in the making of this reactor. Many of the target analytes were volatile organic compounds (VOCs). The tendency for the target analytes to volatilize required that the system for testing the reactor be airtight. All sampling methods and analytical procedures were also focused around this important issue of preventing volatile loss of the analytes.

Several tests were performed during the course of this research with the goal of understanding the reactor's capabilities and the process of photocatalytic oxidation. Tracer analyses were performed to understand the hydrodynamics of the reactor. Adsorption and desorption of the 8 target compounds on the photocatalyst was also examined. UV intensity, empty bed contact time (EBCT), and total oxidation of the contaminants in their original state were considered.

Making of the Silica-Titania Pellets

Pellet Composition

To create the photocatalyst a silica gel matrix was impregnated with TiO_2. The titanium dioxide was contained both inside the gel itself and in the pores of the gel. This

silica/titania gel was made into a pellet form measuring 3 mm in diameter were fixed in a reactor (packed bed style) allowing solutions to pass through the packed bed.

The pellets were designed according to the formula chosen in the research conducted by Danielle Londeree (2002). Ethanol, hydrofluoric acid (HF), nitric acid (HNO_3), Degussa P25 titanium dioxide, water, and tetra-ethyl-orthosilicate (TEOS) make up the list of necessary chemicals for this formula. First, 4.2 grams of TiO_2 were placed in a polymethylpentene jar. Next, an 8 oz. plastic jar was put on a mixer with a magnetic stir bar to keep the solution thoroughly mixed as the contents were added in the following order: 25 mL deionized (DI) water; 50 mL ethanol; 35 mL TEOS; 4 mL HNO_3; 4 mL HF; 4.2 grams TiO_2. All acids were reagent grade. The TiO_2 used in this research was Degussa P25. TEOS and water are the two components that actually make up the silica gel matrix. TEOS, a silicon alkoxide is a specific type of silica precursor. The ethanol allows the TEOS and the water to combine. Nitric acid and hydrofluoric acid are used to speed up the reactions that create the gel. In addition the two acids can be used to alter the pore size and structure within the gel. The water, ethanol, and TEOS were measured using 10 mL graduated glass pipettes and then the acids were introduced through 10 mL graduated plastic pipettes. Figure 3 shows the jars and mixers where the solution gelled for approximately 1 hour before the process of creating the pellet forms was begun.

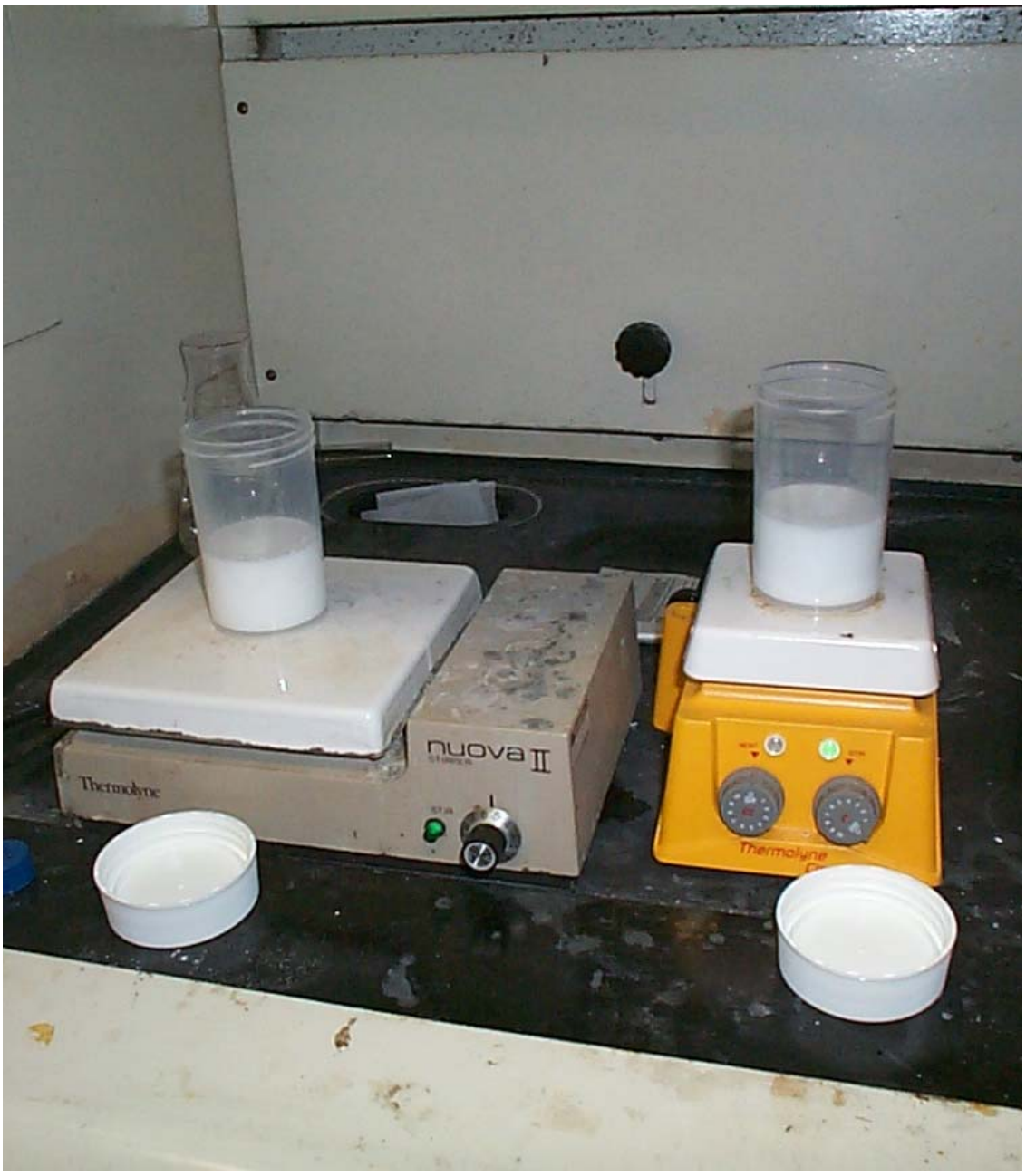

Figure 3. Picture showing an example of the 8 oz. jars, sitting on mixers and filled with the silica-titania suspension, going through the gelling process.

To obtain the pellet shape, the suspension was pipetted using an automatic pipetter into 96-well assay plates. Figure 4 shows a picture of this process. Each batch of chemicals created approximately 4 assay plates worth of pellets. Each batch of assay

plates was then stacked into groups of 4, capped with an assay lid, and wrapped in aluminum foil and duct tape.

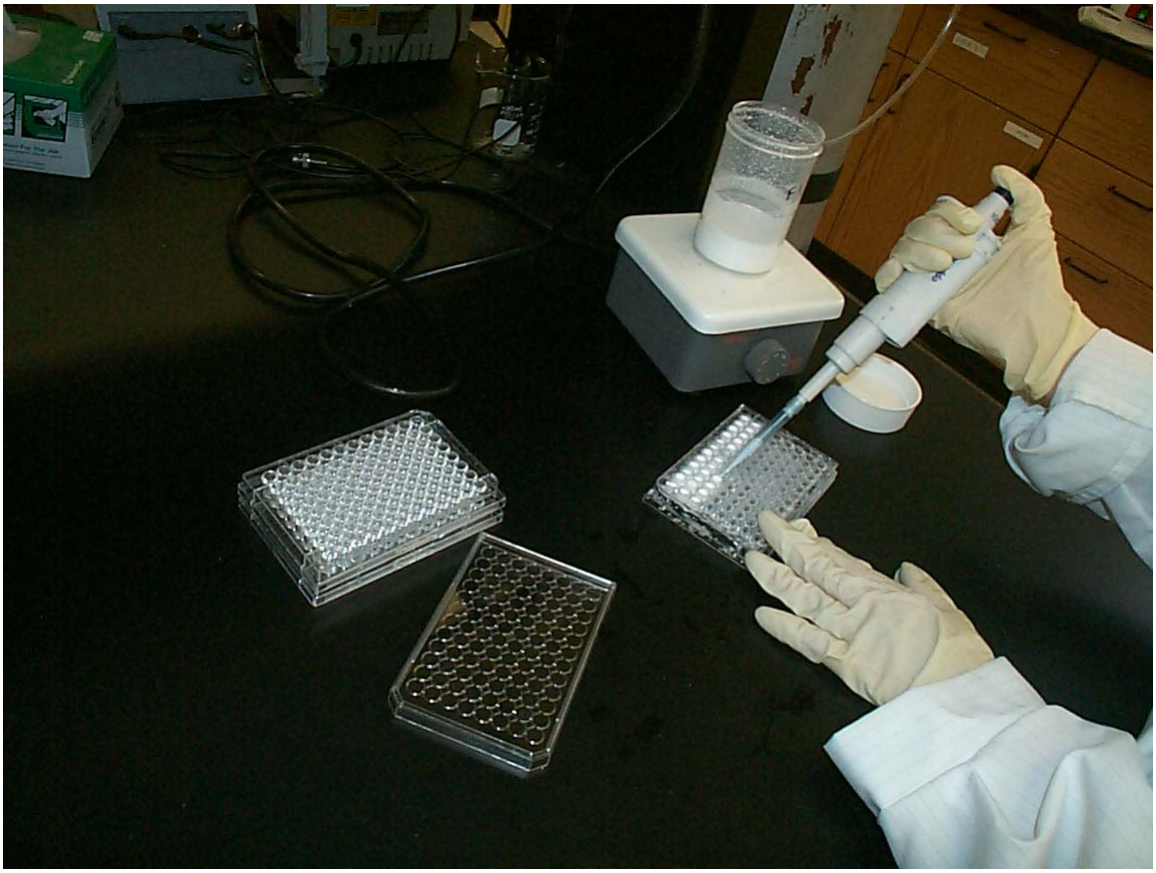

Figure 4. Suspension being transferred from the 8 oz. gelling to the assay plates used for creating the pellet shape.

Aging

After putting the solution into assay plates, the pellets underwent the "aging" process. This is where the fluid is dried from the inside of the pellets, leaving behind the structure that holds the gel together. The aging process used in this research consisted of first leaving the assay plates at room temperature for 48 hours and then moving the pellets to an oven preheated at 66 °C. For 48 hours the gel aged in the 66 °C oven. Pellets were then removed from the assay trays and put into an 8 ounce Teflon jar with a hole in the top for equalizing pressure between the inside and outside of the jar. The jar

was put into a programmable oven that gradually increased the temperature from 25 °C to 103 °C at a rate of 2 °C/min. The jar stayed at the 103 °C temperature for 18 hours. After the 18 hours, the temperature was then increased from 103 °C at the same rate as before to the temperature of 180 °C where it remained for 6 hours before gradually decreasing the temperature back down to 25 °C. The pellets were then removed and placed in plastic jars for storage. A majority of the pellets came out of the oven with a slight brown color. To remove the color, the pellets were put into a ceramic dish and heated in an oven at 500 degrees Fahrenheit for approximately 1 hour. This removed the brownish tinge almost completely. It was also found that over time the brown color would slowly dissipate without the addition of heat. Figure 5 shows a diagram that displays the overall aging process used for creating the photocatalyst used in this research.

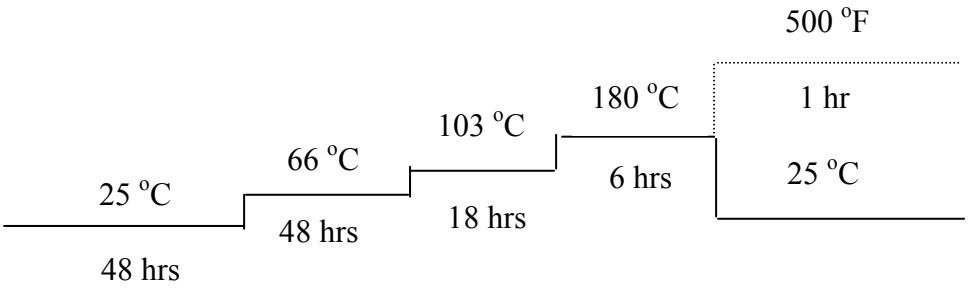

Figure 5. Diagram showing the aging process for the pellets. The dashed line is used for the 500o F to indicate that not all gels required this treatment.

The Reactor

Design of the Reactor

The bench-scale reactor was designed and constructed in order to contain the pellets and provide effective oxidation of organic compounds and inactivation of pathogenic microorganisms. It was necessary to develop a reactor that would be well

suited for photocatalysis and for testing the pellets. One important issue was the transmission of ultraviolet light. Quartz was chosen for its ability to transmit UV radiation energy, as demonstrated by the transmittance of energy at the wavelength of 388 nm shown in Figure 6 (http://www.quartz.com, 2003).

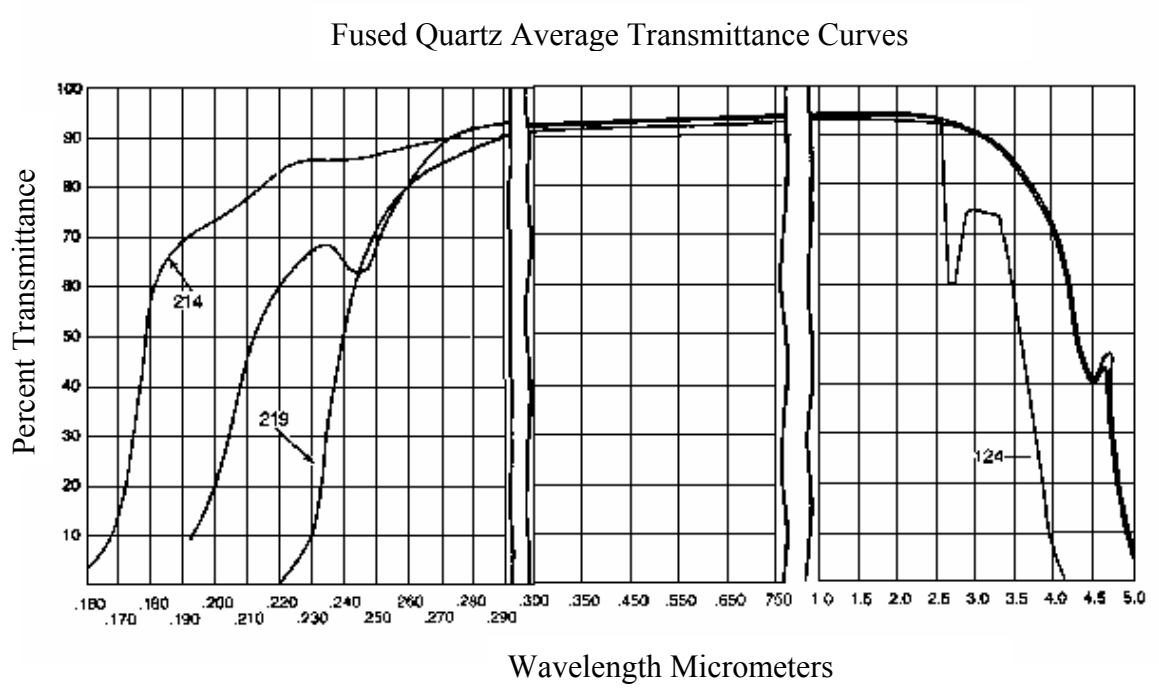

Figure 6. UV transmittance curve for the quartz material used in constructing the reactor.

The reactor shape (Figure 7) was chosen to optimize the exposure of the pellets to the light. By building the reactor in a cylindrical shape to surround the lamps, most of the UV energy produced would be used. It was also important that, should the need arise, the pellets could be easily removed from the reactor. For this reason alternate configurations such as a coil were avoided. The thickness of the reactor (10.5 cm) was chosen to give every pellet inside the ability to react with UV radiation. A thicker reactor would have hid some pellets behind others, thereby creating a waste of catalyst. The

schematic shown in Figure 7 gives the dimensions and shape of the reactor used in this NASA research.

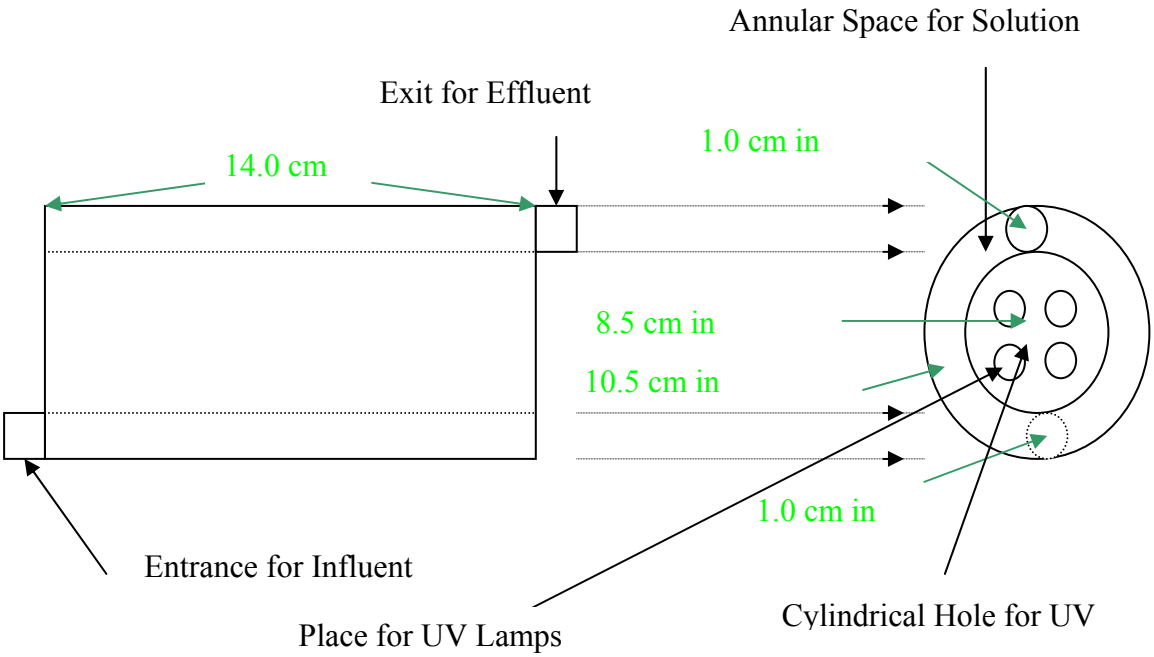

Figure 7. Diagram showing the plans for the dimensions and shape of the reactor used for containing the pellets. The entrance and exit were each given threaded ends to allow for O-Ring connectors. This was done to provide connections for the PTFE tubing used in the system. A frit was placed in the exit port to prevent the pellets from flowing out of the reactor with the solution.

The entire reactor was made of quartz with the exception of one end where a glass frit was placed to keep the pellets from flowing out of the reactor. The reactor had a volume of 436 mL with the pellets taking up 109 mL of that space (the pellets filled the reactor completely, but the remaining 327 mL was interparticle space. The bed porosity was estimated by filling a graduated cylinder with 24 mL of pellets and then adding nanopure water (NPW) until the water was at the same level as the pellets. 18 mL of NPW were added in all. This led to the conclusion of 75% bed porosity within the reactor. Figure 8 shows the reactor in place on its support.

The Reactor System

A system was designed for testing the reactor's capabilities for degrading the target analytes. That system included the reactor and reactor support, two sampling ports, a source tank, a pump, and a flow dampener. Figure 9 shows a schematic of the entire system setup.

The reactor was placed on a wooden support in the horizontal position to limit the influence of gravity on the flow. Since NASA specifications require the reactor to work in a micro gravity situation, it was necessary to keep gravity from enhancing the results of the experiments. Connections were made available for 4 UV lamps to be used in the center of the reactor. The lamps were 12-inch, 8-watt lamps that each provided approximately 4.44 W of available UV energy (wavelength near 365 nm) to the inner surface of the reactor (Table 20). The support also included a cover that could be placed over the reactor and UV lamps to prevent exposure to laboratory personnel.

All of the tubing used was PTFE tubing to prevent adsorption or desorption of organic compounds during experimentation. Several of the target analytes fall into the category of volatile organic compounds (VOCs). Therefore, all connections were sealed with PTFE tape to ensure an airtight system

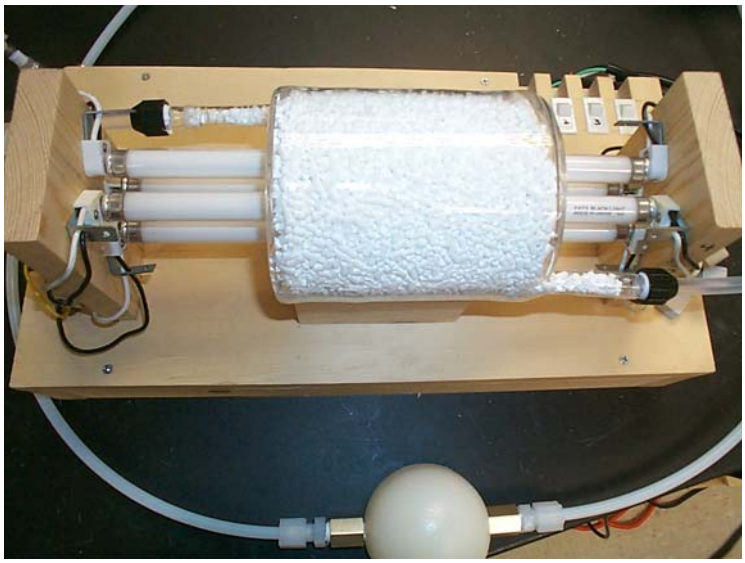

Figure 8. Picture of the reactor on its support stand and connected to the system used for the testing.

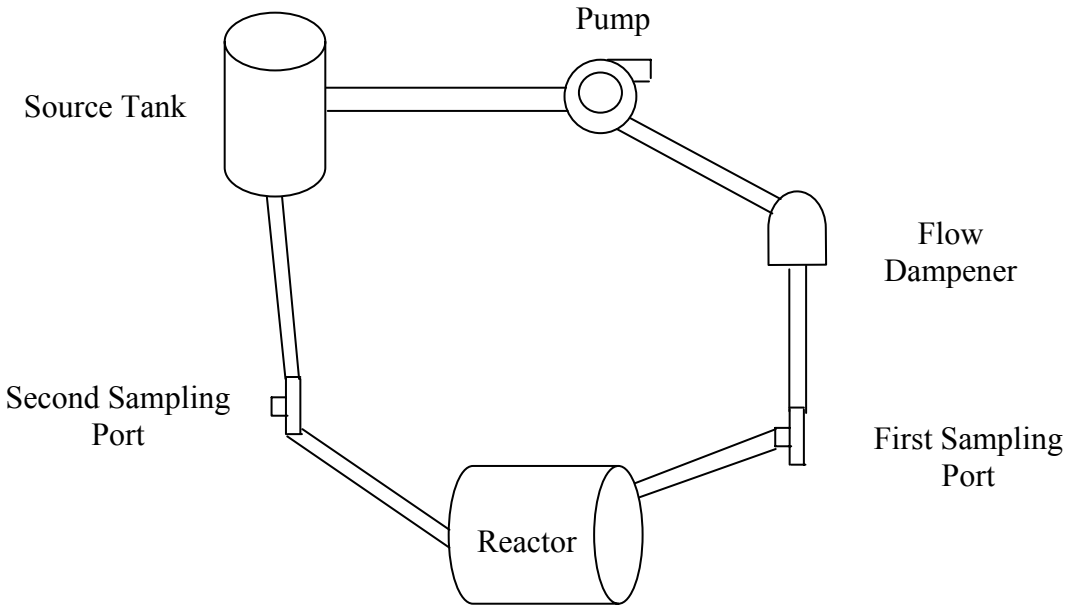

Figure 9. Diagram of the system setup used for testing the reactor's capabilities. The diagram does not show the magnetic stir plate under the source tank. It also does not show the wooden support stand for the reactor. However, that support is depicted in Figure 8.

Since each sample taken from the system was 40 mL, a source tank was necessary to prevent pockets of air from forming in the tubing or in the reactor. A 1 L Erlenmeyer

Figure 10. A picture of the 4 L source tank used in reactor system for this research.

flask was initially used to fill this role. Later in the research the size of the source tank was increased to a 4 L Erlenmeyer flask to further reduce the effects of sampling. Glass rods placed through a rubber stopper on top of the source tank carried solution in and out of the flask. The rubber was covered in Teflon tape to preclude reactions between the stopper and the test solution. One glass tube through the stopper allowed a small air leak to prevent a vacuum situation within the system when samples were taken. This did result in a necessary 14.5 mL of headspace at the top of the flask to keep from losing solution out of that tube. A picture of the source tank is shown in Figure 10. The total volume of the system was a little over 1.5 L (4.5 L with the change in source tank) with 1.3 L (4.3 L) coming from the flask and the reactor. The pump used was a L/S PTFE-

Tubing Pump Head powered by a L/S Variable-Speed Modular Drive. A polyethylene pulse dampener was used to ensure a steady flow rate in the system.

Reactor Hydrodynamics

All real reactors behave, from a hydrodynamic perspective, in a range between two ideal reactor types. Those two ideal types are known as a continuously stirred reactor (CSTR) and a plug flow reactor (PFR). A CSTR represents the ideality where the entire reactor is completely mixed and the concentration in all locations within the reactor is the same as the effluent concentration. A PFR allows for no axial mixing (mixing in the direction of flow) and therefore a concentration gradient exists from the influent to the effluent of the reactor. The PFR is representative of an infinite number of CSTRs in series. No working reactor can ever operate completely as one of these ideal reactors, but every reactor behaves somewhere between these two ideals.

The goal was to design a reactor that would simulate a PFR as closely as possible. A PFR was desired to maximize the reactor's performance as a PFR provides the greatest transformation for all positive order reactions. This would lead to a predictable and reliable reaction rate and a minimum size for the reactor to achieve a selected degree of oxidation or disinfection.

In order to determine the hydrodynamic behavior of the reactor, a tracer analysis was performed. Sodium chloride (NaCl) was chosen for the tracer to prevent any possibility of staining the pellets or the inside of the reactor, which may have led to a reduced transmittance of UV radiation. Also, NaCl was not expected to react with the pellets in the reactor system.

The chosen flow-rate for the tracer analysis was 10 mL/min since this was the design flow for the reactor. With a reactor volume of 436 mL and 109 mL of that composed of pellets, the mean residence time of the reactor was predicted to be 32.7 min.

The tracer analysis was conducted by first maintaining a steady flow through the system of DI water at 10 mL/min. A solution of 2 mg NaCl/mL was put into a gas-tight luer-lock syringe. An aliquot of 5 mL of that solution was then introduced through a luer-lock connection into the tubing. The tubing leading from the sampling port to the reactor created about 3.7 min of plug flow time prior to entering the reactor.

The concentration of NaCl in the effluent was measured using a Fisher Scientific conductivity probe. The probe constant, as determined in a calibration procedure (Standard Methods, 2000), was 0.866. This was calculated by preparing concentrations of potassium chloride, which were known to have specific conductivity (Table 18). Then the readings of the probe were compared against those standard values. 3 readings were taken and from those readings an average difference between the actual conductivity and the real conductivity was calculated. That average difference was then divided by the actual conductivity to determine the probes cell constant of .866. This means that any conductivity reading on the probe actually corresponded with 0.866 mmhos/cm of that reading.

A linear correlation was found between the conductivity reading on the probe and the concentration of sodium chloride in solution from 0 to 576 mg/L. This was done by measuring known concentrations of sodium chloride and comparing them with the reading on the probe. This showed that each mmho on the probe represented 0.562 mg/L of NaCl in the solution (Figure 29).

Using this information, data from the tracer analysis were collected in the form of conductivity in the reactor effluent over time. The conductivity was then changed to a concentration of NaCl. Samples were taken of the reactor effluent prior to injection of NaCl in order to determine the natural conductivity in the effluent. The average conductivity was subtracted out so that only conductivity caused by the tracer analysis impulse was considered. The mean residence time in minutes, variance, and tanks in series were calculated. These numbers are displayed in Table 3. The residence time represents the average amount of time sodium chloride remained in the reactor. Variance describes the difference in times over which the contaminant left the reactor. Also calculated, was the number of CMFRs in series. This shows how many CMFRs in a row it would take to create a residence time distribution like the one seen by the reactor. An infinite number of CMFRs in series represents a plug flow reactor.

Table 3. Key Statistics from the Tracer Analysis

Mean Residence Time	42.07
Variance	458.94
Number of CMFRs in Series	3.86

E-curves (residence time distributions) were generated, based on the data, to graphically demonstrate the results of the tracer analysis. The Tanks in Series (TIS) model was used due to its ability to accurately model the reactor. Figure 11 shows the E-curve produced. The ability of the TIS model to simulate the flow in the reactor is key to the calculation of reactor kinetics discussed later in the results section of this thesis.

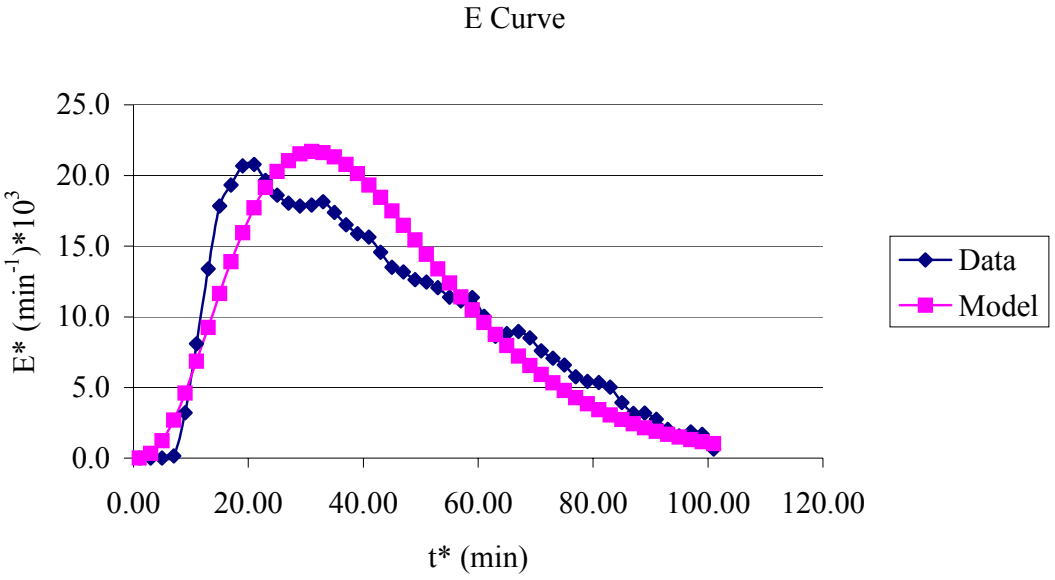

Figure 11. E curve generated using the data from a tracer analysis performed on the reactor used in this research. The data represent the E-curve actually generated by the reactor. The model curve is the E-curve generated by the TIS model.

Sample Collection

Samples (with the exception of those in the desorption experiments) were collected using a gas tight, luer-lock syringe. Samples were taken from one of the two three-way luer-lock sampling ports provided in the system. Volatile Organic Analysis (VOA) vials were used to collect the samples and keep them airtight. Each vial was 40 mL. These vials were stored in refrigerators at 4^{o} C until they could be analyzed. Each sample was viable for up to two weeks at that temperature.

Sample Analysis

Samples were analyzed using two different methods, one for acetone, carbon disulfide, chlorobenzene, ethyl acetate, methyl methacrylate, and toluene, and a second method for butyl alcohol and indole.

The first method of analyses was performed using a GCQ gas chromatograph/ mass spectrometer with a Tekmar 3100 purge and trap extraction system. Analyses were performed in accordance with the USEPA method 524.2, Methods for the Determination of Organic Compounds in Drinking Water: Supplement 2 (USEPA, 1992). Samples were purged at room temperature for 11 minutes at 35 mL/min with helium. They were then dry purged for 2 minutes to remove water. The Supelco k-trap was then back flushed and heated to 250 °C for desorption to the column. The column used was a DB-VRX column from J&W Scientific. It was a 75-meter long column with a 0.45 mm inner diameter, and a 2.55-µm-film thickness. Desorption to the column lasted for 6 minutes at the 250 °C and the trap was then baked at 270 °C for 10 minutes. The column was taken from a 25 °C start temperature and ramped to 220 °C at a rate of 6 °C/min. An initial hold was done at 35 °C for 6 minutes. The mass spectrometer used is an ion trap that looks between 34 amu and 280 amu with 0.6 seconds/scan.

The second method of analysis (for butyl alcohol and indole) was performed using a Hewlett Packard 5890 GC/FID with a solid phase micro extraction (SPME) process using a StableFlex Divinylbenzene/Carboxen/PDMS fiber. Analyses were performed in accordance with an alternative of AWWA Method 6040D, Analysis of Taste and Odor Compounds by SPME. Samples were adsorbed to the fiber for 15 minutes at 100 °C. They were then desorbed to the column by increasing the temperature from 45 °C where it was held for 5 minutes to 220 °C where it remained for 7 minutes. The rate of temperature increase was 15 °/min.

The reliability of the testing was verified using the % Relative Standard Deviation (%RSD). %RSD is based on the Response Factor (RF) of a chemical. The RF and %RSD are calculated using Equations 12 and 13.

$$\text{Response Factor (RF)} = (\text{Area}_{\text{analyte}} * \text{Amount}_{\text{internal standard}}) / (\text{Area}_{\text{internal standard}} * \text{Amount}_{\text{analyte}}) \quad \text{(Eq.12)}$$

$$\text{\% Relative Standard Deviation (\%RSD)} = 100 * (S_{RF} / RF_{AVE}) \quad \text{(Eq.13)}$$

The USEPA method requires a %RSD of less than 30, but strongly recommends a %RSD of less than 20. Table 4 gives the average %RSDs for the analyses performed for this research.

Table 4: Average %RSDs for the Analyses in this Research

Chemical	Average %RSD
Acetone	32.5
Carbon Disulfide	23.8
Chlorobenzene	13.9
Ethyl Acetate	13.1
Methyl Methacrylate	11.4
Toluene	18.6

Performing Experiments

Initial Degradation

An initial test was performed to determine if the reactor would demonstrate the capability for removing the target compounds. This experiment was performed using the system in the configuration shown in Figure 9. The only difference was that at this time the second sampling port did not exist. That was added later in the research.

A solution containing the 8 target analytes (acetone, butyl alcohol, carbon disulfide, chlorobenzene, ethyl acetate, indole, methyl methacrylate, and toluene) was prepared using the following steps:

- 1-2 μL of each of the 8 neat chemicals were added to a 50 mL volumetricflask.

- The volumetric flask was inverted five times for mixing.
- 20 mL of solution from the 50 mL flask was added to a 2 L volumetric flask already containing 2 L of deionized (DI) water.
- This larger flask was then inverted 5 times for mixing purposes.

The prepared solution was then carefully poured into the source tank used in the system to minimize volatilization. Solution was pumped through the system until all of the tubing and reactor were filled. The source tank was then refilled back to the top and the stopper replaced.

12-inch, 8-watt UV lamps were then placed in the center of the reactor. They could not be placed prior to filling because the reactor had to be tilted in order to ensure it would fill completely. The lamps were shielded using aluminum foil and turned on to warm-up. A support cover was used to prevent the exposure of laboratory personnel to UV radiation.

For the rest of the experiment the contaminated solution was circulated through the system at a rate of 10 mL/min. After thirty minutes of time allowed for the lamps to come to full intensity, the foil shield was removed to allow photocatalysis to begin. A sample was taken here representing the initial ($t = 0$) concentration for the analytes before any photocatalysis took place. Samples were then taken every 2 hours for the next 6 hours. After the 6 hours the lamps were turned off and the system drained.

Figure 12 displays the results of this initial degradation experiment. The results of the experiment show removal of contaminants from the solution. All 3 of the contaminants shown in Figure 12 demonstrated a better than a 90% removal over the course of the 6-hour run. The capability for the reactor to remove NASA's target analytes was demonstrated in this experiment.

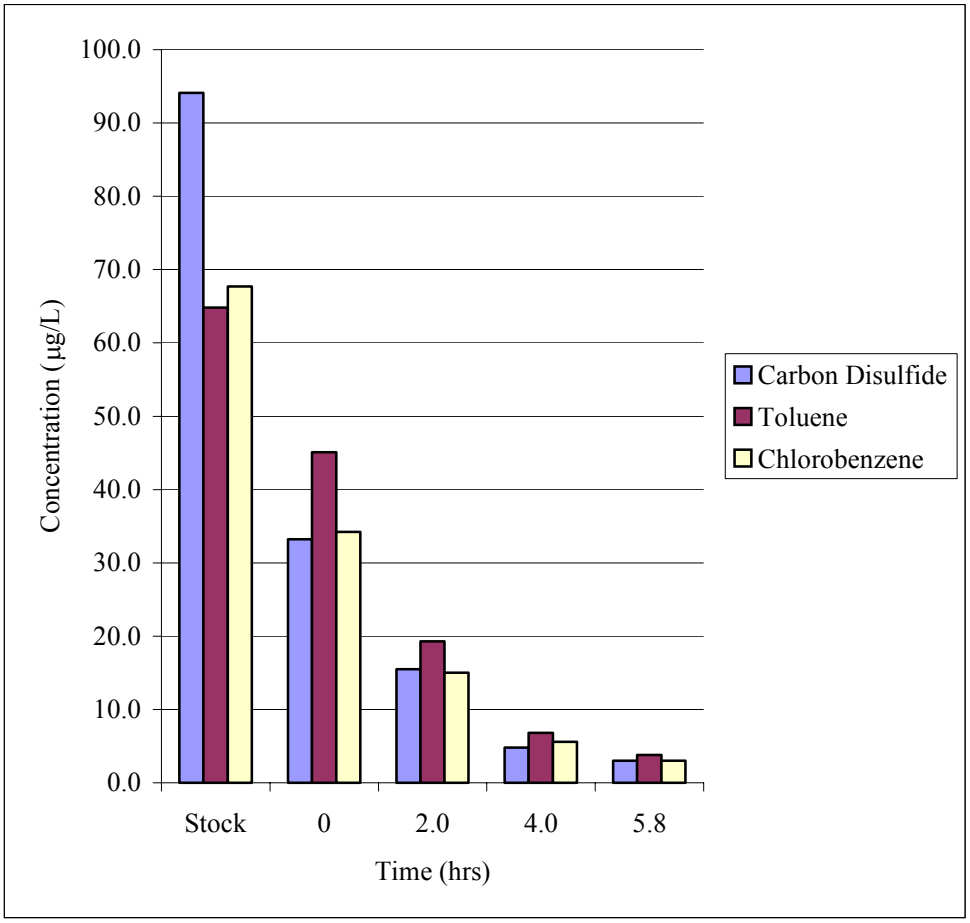

Figure 12. Target analyte degradation seen as a result of recycling the spiked solution through the system. 3 of the 8 target analytes are displayed in this figure. The data represented in the "Stock" bars represents the initial concentration prepared in the 2-liter volumetric flask. The "0" data is the concentration measured after the system containing the 1-liter source tank was filled.

Determining Effects of Volatility

Three sources of loss were anticipated in the experiments. Work indicated that in this experiment some loss was probable due to volatilization, some to adsorption on the pellets, and the rest due to photocatalysis. Many measures were taken to reduce volatility losses in the system. Teflon tubing, stainless steel connectors, and Teflon tape at each junction were all used in an effort to reduce this loss. Other measures of protection against volatility included the use of gas-tight syringes, luer-lock sampling ports, and keeping the headspace in the source tank at a minimum.

Losses due to adsorption were expected and encouraged. Adsorption loss was considered a viable means of contaminant removal for the NASA analytes. However, adsorption losses had to be accounted for, because adsorption removal was finite and could not be relied upon for an entire space mission to Mars (the eventual goal of this reactor). It had to be proven that after the pellets adsorption capacity was exhausted, photocatalysis alone would have the capability of sufficiently removing the analytes.

An experiment was performed to ensure that losses of analytes were not due to volatility. For this experiment the reactor was taken out of the system setup. A schematic of this setup is shown in Figure 13.

The solution for testing was prepared in accordance with the same method described for the initial degradation experiment. Solution was then added to the source tank and pumped through the system to fill up the tubing. As before, the source tank was filled to the top and capped with the rubber stopper. For 8 hours, the contaminated solution was allowed to circulate through the system at a constant flow rate of 10 mL/min. Samples were taken every two hours for analysis. The results of this experiment are shown in Figure 14.

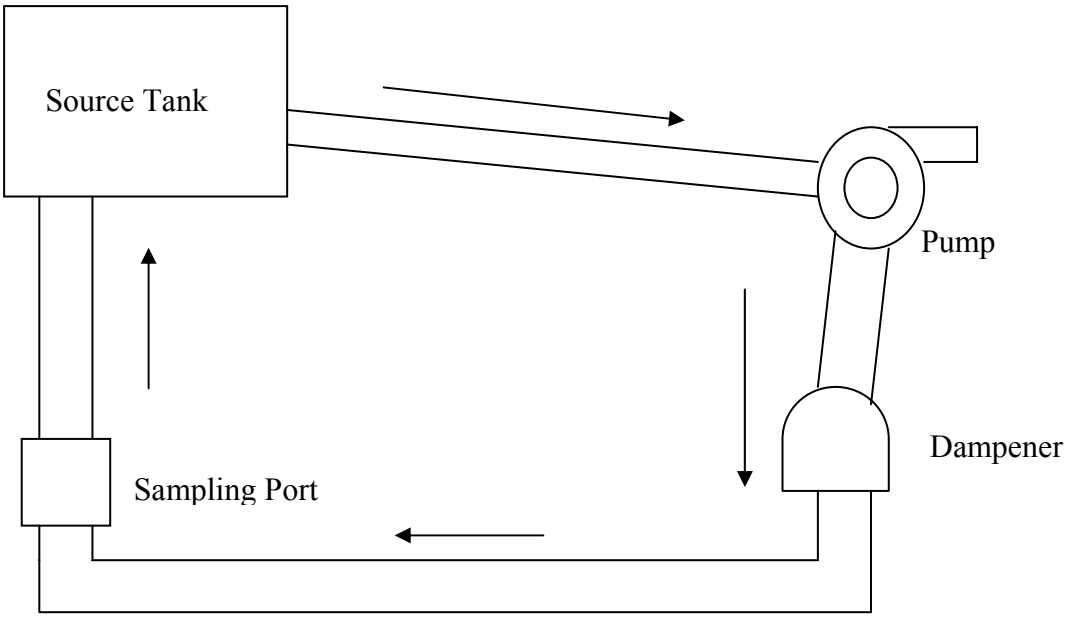

Figure 13. Diagram demonstrating the setup used for estimating volatile losses of analytes in the system. Only one sampling port is shown in the diagram because only the first sampling port was online during this experiment.

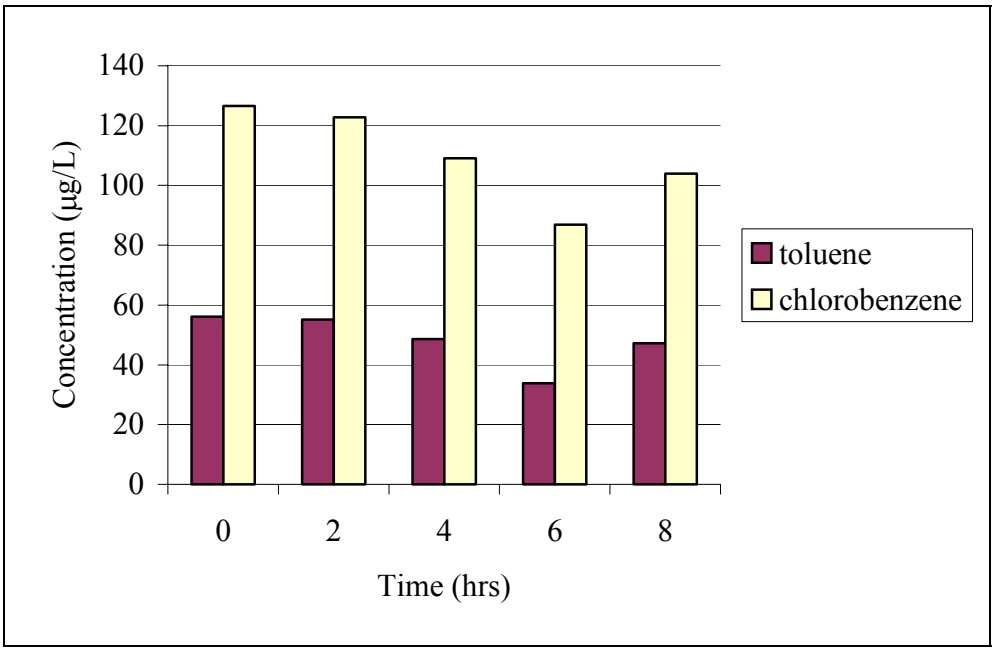

Figure 14. Volatile losses in the system over an 8-hour period without the reactor in place. Samples were taken every 2 hours from the 1st port in the system. This run was performed with a 1-liter source tank, making the entire volume a little over 1.1 liters.

Figure 14 shows small volatile losses for both chlorobenzene and toluene (16% and 18% respectively) over the 8-hour period of the experiment. The results of analyses for the 6-hour sample appeared to be anomalous and may have been affected by reloading the feed tank at about this sampling time. Discounting the 6-hour sample, volatility losses over an 8-hour period were 16% and 18% for toluene and chlorobenzene, respectively. After this experiment certain measures were taken to try to further reduce volatility. This included reduction in headspace for the feed tank and a more secure wrapping of PTFE tape around the rubber stopper. Based on this experiment and the further measures taken, volatile losses were assumed to be negligible in future experiments.

Adsorption Experiment

Following the volatility test, adsorption became the next source of loss to isolate. The system was reconfigured to that shown in Figure 15.

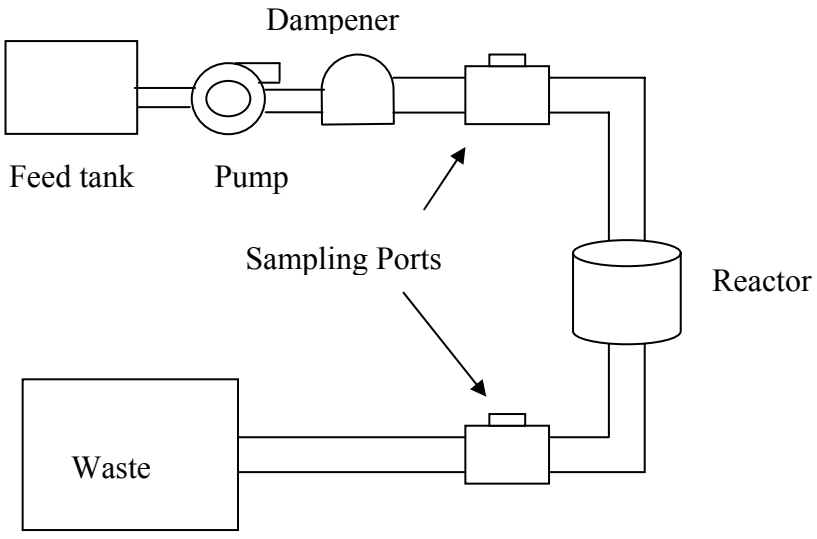

Figure 15. Diagram showing the setup used for saturating the catalyst pellets.

Using the setup shown in Figure 15, 8 liters of contaminated solution at approximately 200 µg/L was put through the reactor with the lights off. This was done to ensure that adsorption would not be a cause for loss of analytes in the rest of the research.

To assess losses by adsorption, an experiment was run with the setup in the configuration shown in Figure 15. Solution was prepared and introduced to the system using the method described in Initial Degradation section. The solution was circulated through the system at 10 mL/min for 5 hours. The lamps were left on but shielded during this experiment to keep the conditions similar to what the reactor would typically experience. Samples were taken every hour over the 5-hour period to determine the rate at which the concentration changed. The results of this experiment are shown in Figure 16.

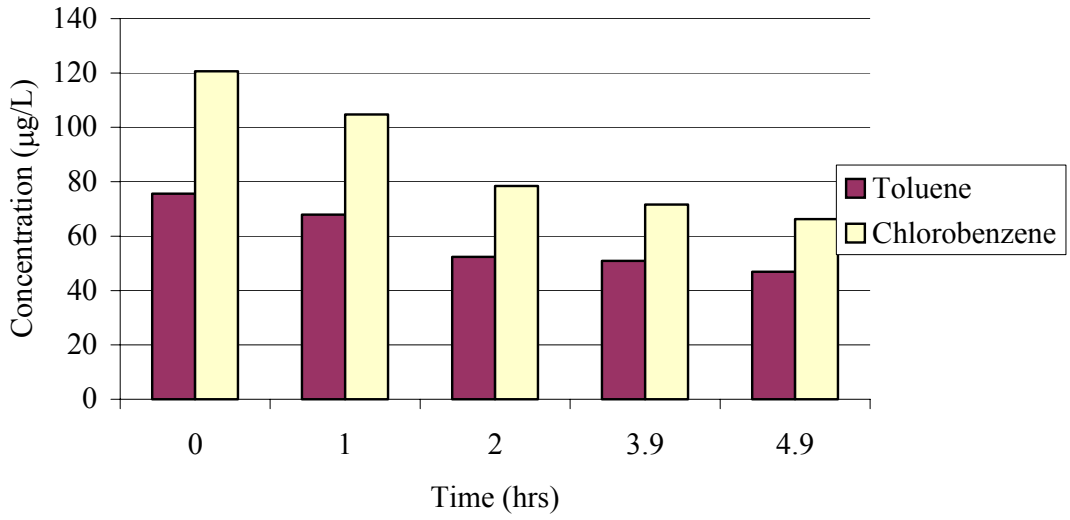

Figure 16. Loss of toluene and chlorobenzene as a result of adsorption in the reactor system. The source tank was excluded from the experiment as any adsorption there was predicted to be minimal. The "0" sample represents the concentration after addition of contaminated solution to the system.

This graph shows that some loss is still being experienced in the absence of photocatalysis. However, it can be seen that the loss becomes minimal as the concentrations begin to level out by the fifth hour. Based on this experiment, the decision was made to operate future experiments by letting the system run for five hours prior to beginning the photocatalysis experiments. At this point all losses would be considered due to photocatalysis only.

Desorption Experiments

Experiments were conducted to study desorption of the target analytes from the catalyst pellets occurring in the reactor. Contaminated solution was prepared according to the method described in the Initial Degradation section. The reactor system was then filled with solution and allowed to circulate at 10 mL/min for 5 hours. This was done to saturate the gels with respect to adsorption. At the end of the 5 hours a sample was taken and the system was drained. 300 mL of nanopure water was then put through the system to rinse the extraparticular space within the reactor. This rinse water was then analyzed to determine the concentration rinsed. Nanopure water was then put into the entire system, with the source tank excluded, to allow for possible desorption. The period of exposure chosen was 45 minutes. After exposure to the nanopure water for this duration, the system was drained into a 500-mL volumetric flask and the flask was inverted to provide mixing (excess solution from the system was wasted). Two samples were taken from the 500-mL flask for analysis. In a second test the solution was allowed to remain for another 23 hours and 15 minutes after the 45-minute sample. The system was then drained and a sample was taken to represent 24 hours of desorption.

The data in Figure 17, representing the results of the two desorption experiments, led to two important conclusions. The first conclusion was that the contaminants do

desorb from the silica/titania gels pellets. This means that when low-level concentrations (lower than those seen in Figure 17) are seen in future experiments the photocatalysis has to degrade contaminants in the feed solution as well as the contaminants that are desorbed from the silica gel-titania composite.

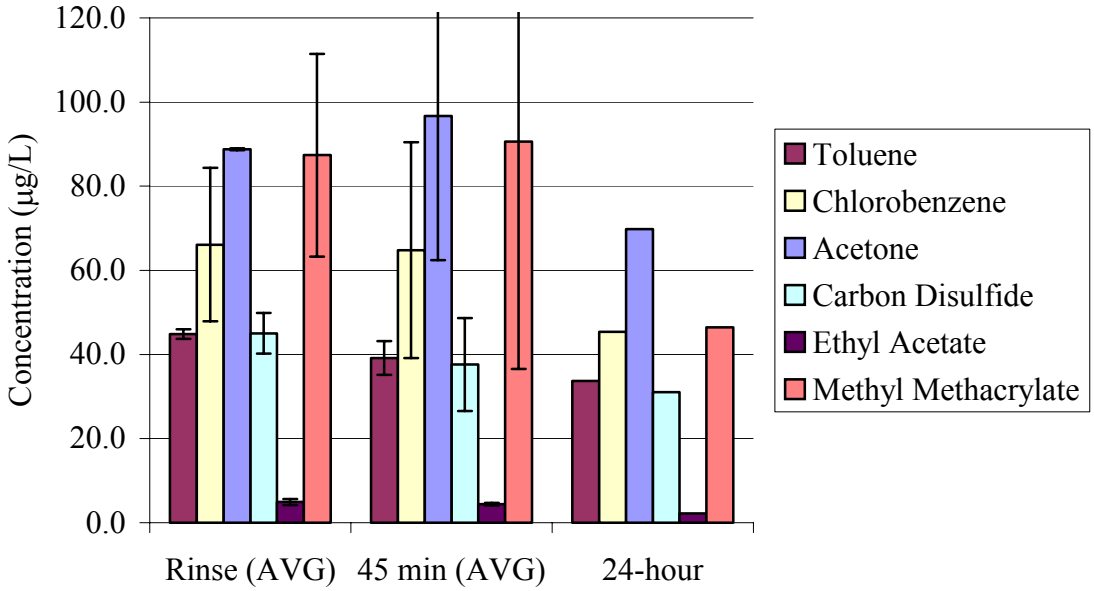

Figure 17. Results of desorption experiments performed. The Rinse (AVG) columns represent the average concentration in the rinse solution sample over two experiments. The 45 min (AVG) columns represent the average concentration of contaminant in the NPW solution after 45 minutes of contact with the reactor. The 24-hour columns represent the average concentration after 24 hours of circulating through the system. Error bars are representative not of the error in 1 experiment, but the range of data in the 2 separate runs.

Oxygen as an Electron Acceptor

Photocatalysis requires the continual presence of an electron acceptor. When UV radiation comes in contact with the TiO_2 surface it creates an excited electron and a hole left behind by the electron. In the absence of an electron acceptor the excited electron would simply recombine with the hole leaving no ability for hydroxyl radicals to be

formed. Oxygen is the most prominent acceptor available and also the cheapest available to fill the position in the NASA research.

To demonstrate the availability of oxygen for use as an electron acceptor in the NASA reactor, an experiment was performed. The setup was configured to that shown in Figure 8. The method outlined in the Initial Degradation section was then followed for this experiment, with a small exception. Before the lamps were turned on, the solution was allowed to circulate for five hours in order to let adsorption effects take place. From then on the lamps were turned on for 6 hours. For this case, samples were only taken of the oxygen concentration in the influent solution and of the final solution at the end of photocatalysis.

The results of the samples showed no change in the dissolved oxygen level of the solution from the stock solution to the final sample. In both cases the dissolved oxygen level was 5.4 mg/L. This suggests that the concentration of pollutants being degraded in the NASA research is too low to cause a measurable effect on the dissolved oxygen concentration in the system. Based on these results, addition of oxygen or other electron acceptors for wastewater degradation in this research may not be necessary if the dissolved oxygen concentration in the influent contains appreciable levels of dissolved oxygen, as the same level of degradation will be achieved with the currently available electron acceptor concentration. However, tests would actually be necessary with NASA's wastewater from within their process treatment train in order to determine if oxygen would be limiting at very low levels of dissolved oxygen.

Photocatalytic Oxidation Experiments

Effects of UV radiation intensity

Experiments were performed to determine the impact of increasing the amount of UV radiation on degradation of the analytes. Each experiment was performed using the setup shown in Figure 9. Solutions containing between 70 and 200 μg/L were prepared using the method described in the Initial Degradation section. The system was then filled with solution and allowed to circulate at 10 mL/min. Initially, the lamps were left off. Based on results from the adsorption experiment, the solution was circulated for 5 hours before allowing exposure to UV radiation. The lamps were turned on with shields in place at 4.5 hours to provide 30 minutes for the lamps to come to full intensity. At this point, the system was run for 6 hours with the lamps on to allow photocatalysis to occur. Samples were taken every 2 hours for analysis.

This experiment was performed four separate times; once with 3 lamps, once with 1 UV lamp, and twice with 2 UV lamps to assess precision of the data. Table 20 shows the calculations performed to find the amount of energy provided to the reactor by 1 UV lamp. Measurements were made using a Fisher Traceable UV Light Meter. Those measurements contained a possible 2% error on the part of the meter.

Effects of contact time

Experiments were performed to investigate the impact of flow rate on the degradation of the target analytes. Three different flow rates were tested; 10 mL/min, 20 mL/min, and 60 mL/min. Solution for these experiments was created using the method described in the Initial Degradation section. The system was then configured to the setup shown in Figure 8 and loaded with the solution. For 5 hours the solution was circulated to allow adsorption to take place. After 4.5 of the 5 hours, the lamps were turned on and

shielded to allow them to warm up. Thirty minutes later the shields were removed and the system setup was reconfigured to that shown in Figure 11. Flow in the system was changed to 10 mL/min, 20 mL/min, or 60 mL/min for the each of the three different experiments. One liter of solution was put through the reactor at the experimental flow rate. At the end of that time, samples were collected for analysis from the port before and the port after the reactor.

All three of the flow rates tested were within the laminar region of flow as shown in Table 19. This was acceptable since the flow rate NASA predicted of 116 mL/min also lies within the laminar flow regime (Lange and Lin, 1998). So, turbulent versus laminar flow did not have an effect on the flow optimization experiments.

Experiments including indole and butyl alcohol

All of the previously described experiments, the flow optimization, UV optimization, 23-hour experiments, and desorption tests were performed with only acetone, carbon disulfide, chlorobenzene, ethyl acetate, methyl methacrylate, and toluene as the analytes. Tests had to be performed using indole and butyl alcohol as well. These tests required a different method of analysis in addition to the typical GC/MS with purge and trap extraction. Indole and butyl alcohol were analyzed using the GC/FID with solid phase micro extraction (SPME). Samples were collected for analysis of the butyl alcohol and indole using the same protocol as with those collected for the other contaminants, however, the same vial of solution could not be used for both analyses. Therefore, two sample vials were filled at each sampling time.

These experiments were performed in two different ways. The first three were performed in the same manner as the UV optimization experiment using 3 UV lamps and a recycle mode system. The only difference was that indole and butyl alcohol were

included in the stock solution. Two separate experiments were also performed using a similar method to that used in the flow optimization experiments. Five hours of adsorption circulation was performed and then the system was reconfigured to the single-pass system. After 1 L of solution flowed through the reactor, two samples were taken at each port.

CHAPTER 4
RESULTS

This chapter will discuss the results of experimentation to determine the photocatalytic capabilities of the reactor. The effects of UV radiation intensity and empty bed contact time (EBCT) will be considered. It will be proven through the data that all of the target analytes used in this research (acetone, butyl alcohol, carbon disulfide, chlorobenzene, ethyl acetate, indole, methyl methacrylate, and indole) are capable of undergoing photocatalytic oxidation. Rates for the process of oxidation will also be considered based on data from the tests studying the effects of EBCT.

Effects of UV Radiation Intensity

Experiments were performed to investigate the improvement in degradation as the number of lamps was increased. Four experiments were performed using 1 UV lamp, 2 UV lamps, 3 UV lamps and a duplicate for the run using 2 UV lamps. The details of the experimental method are discussed in the Methods chapter (Effects of UV radiation intensity). Figures 18-21 show the results from the UV optimization experiments.

The results from these four experiments demonstrated several important points about the capabilities of the reactor. First, they proved the ability of the reactor to photocatalytically degrade each of the 5 compounds (carbon disulfide, chlorobenzene, ethyl acetate, methyl methacrylate, toluene) shown in the figures. In all cases, at least 80% destruction of the initial contaminant concentration was achieved. Second, the destruction did not appear linear over time, but rather appeared to approach the 10 μg/L

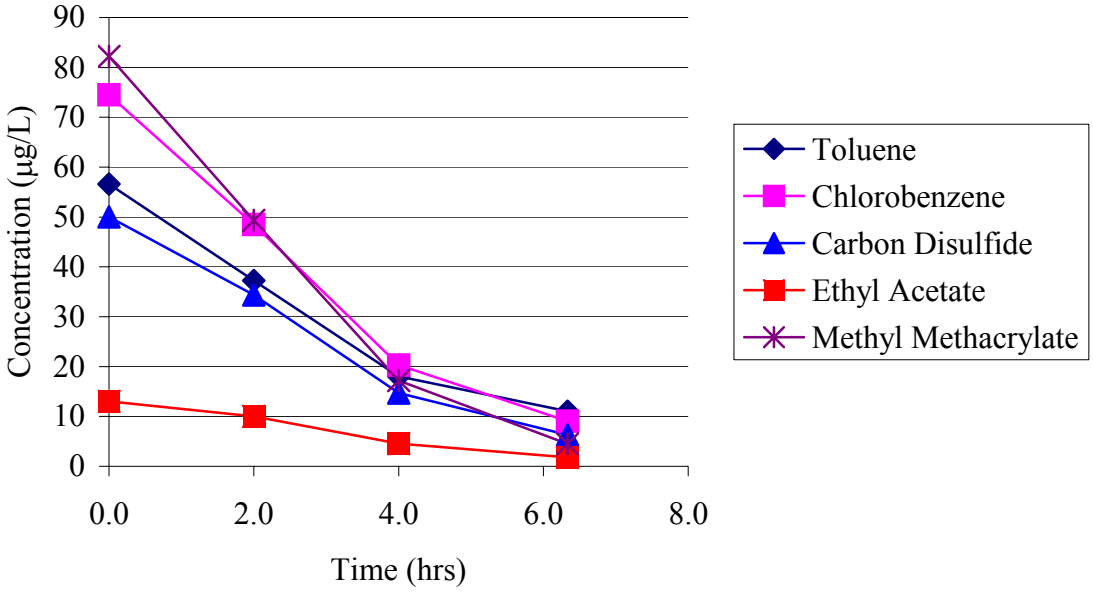

Figure 18. Degradation of 5 NASA target analytes. This loss is due solely to photocatalytic destruction. 3 UV lamps were turned on during this experiment and the experiment was performed in a circulation mode with a 1-liter source tank.

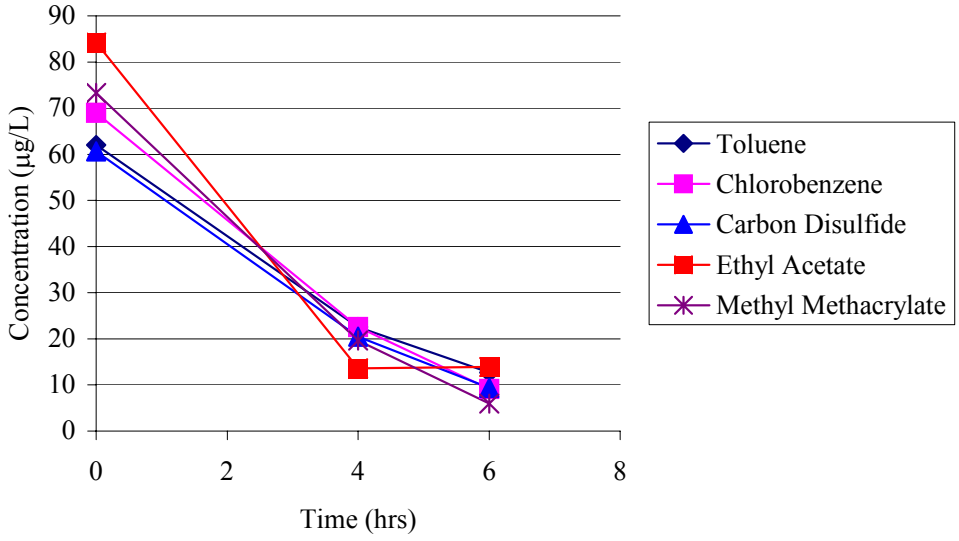

Figure 19. Degradation of 5 NASA target analytes. This loss is due solely to photocatalytic destruction. 2 UV lamps were turned on during this experiment and the experiment was performed in a circulation mode with a 1-liter source tank.

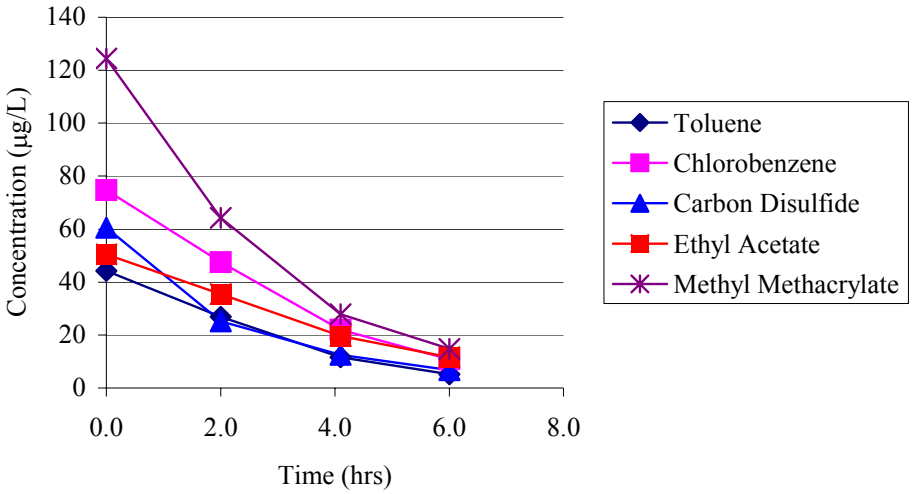

Figure 20. Degradation of 5 NASA target analytes. This loss is due solely to photocatalytic destruction. 1 UV lamp was turned on during this experiment and the experiment was performed in a circulation mode with a 1-liter source tank.

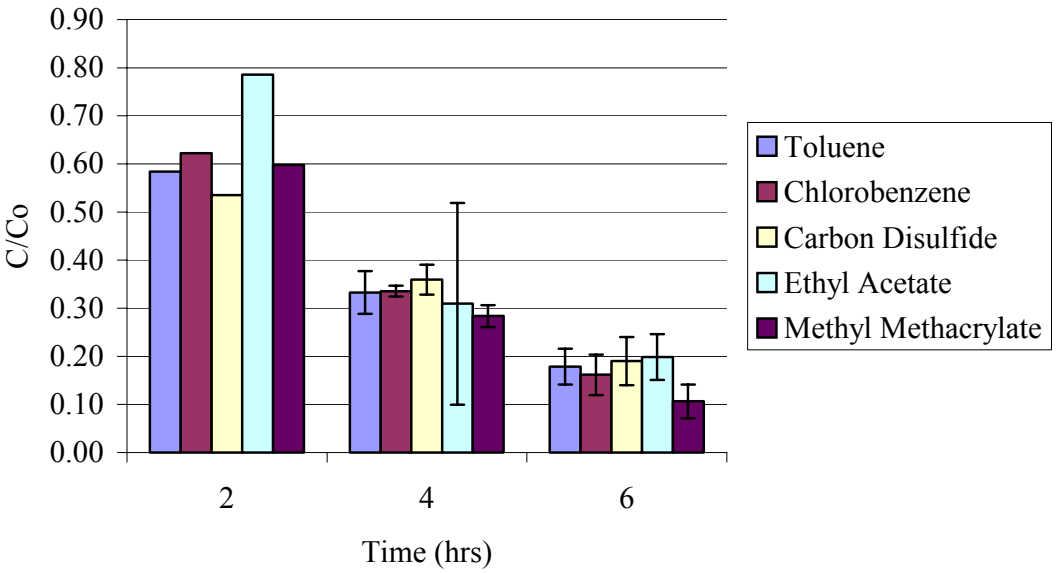

Figure 21. Average normalized degradation seen in the two experiments performed with 2 UV lamps and a 1-liter source tank. Error bars show the range of data for two experiments. There are no error bars present in the 2-hour sample results due to analytical errors in the 1st of the 2 experiments.

concentrations for all of the tests and contaminants. This suggested that the reaction was limited by the ability of the hydroxyl radicals to contact the contaminants, as suggested by the Langmuir-Hinshelwood equation.

Figure 22 shows the normalized curve for chlorobenzene. This curve is representative of the normalized graph for all compounds. The graphs for the other compounds can be found in Figures 29-32. The graph shows all 4 of the UV optimization tests degrading the chlorobenzene at virtually the same rate and magnitude. These data were important to the NASA research because it showed that UV radiation energy was not a limiting factor in the degradation of the target analytes beyond the use of 1 UV lamp. The lower the energy requirements, the more practical the process is for NASA.

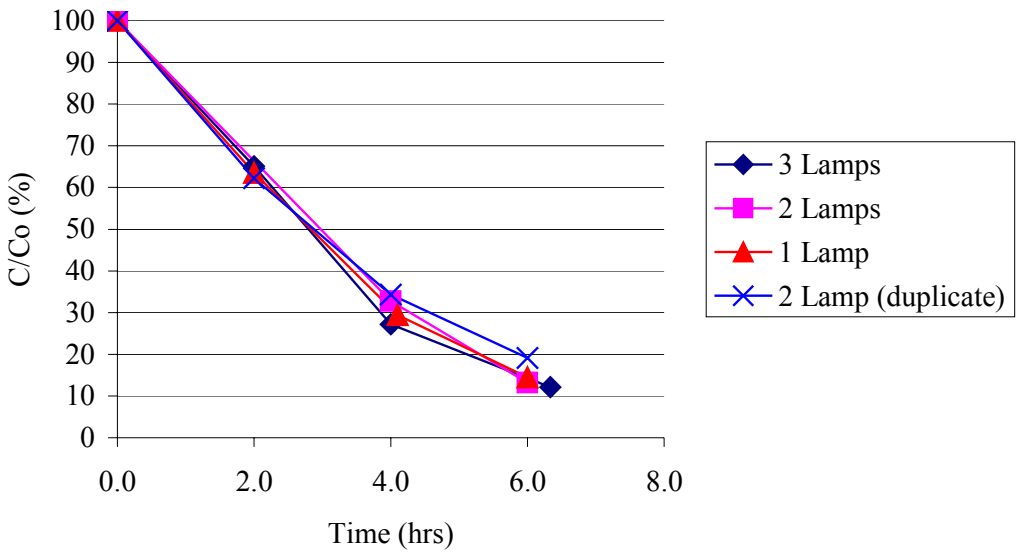

Figure 22. Removal of chlorobenzene is shown over the course of time as a function of the contaminant remaining divided by the initial concentration introduced to the reactor displayed as a percent. It is important to note that the time displayed on the bottom represents time in the overall system rather than just time in the reactor.

Effects of Empty Bed Contact Time

In order to determine the possibility of flow rate and therefore residence time influencing the reactor's performance, a series of experiments were performed. The reactor was studied at three empty bed contact times (EBCT), 7.27 min, 21.8 min, and 43.6 min. These empty bed contact times were achieved by varying the flow rate at 60 mL/min, 20 mL/min, and 10 mL/min respectively. The method used for performing these experiments has been previously described in the Methods chapter (Effects of empty bed contact time). Experiments were performed twice at each of the flow rates. Figure 23 shows the percent of selected contaminants that remain after a single pass through the reactor with the chosen EBCTs. The bars in Figure 23 represent the average value of the two replicates and the error bars represent the range of the data. All of the series raw data can be found in Tables 21-42.

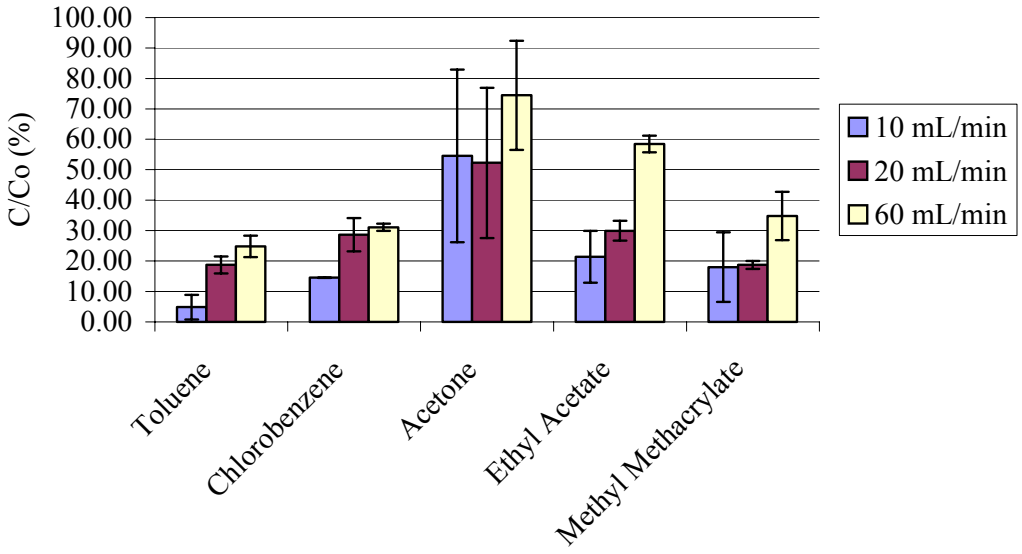

Figure 23. Average results of two flow optimization experiments. The y-axis is given as the concentration remaining in the effluent solution divided by the concentration present in the influent, displayed as a percent. Therefore the smaller columns represent a greater percentage of contaminant removed. % RSDs for acetone were outside of the acceptable range, which explains the large error bars.

The EBCT for solution in the reactor was decreased from 43.6 minutes to 21.8 minutes to 7.27 minutes. A decreased retention time available for photocatalysis should have logically led to a poorer degradation. This hypothesis is proven by the data in Figure 23 where the greater degradation is consistently seen in the tests performed at the slower flow rate.

Not only do the data reported in Figure 23 give insight into the effect of flow rate on the reactor's capability to degrade the target analytes, but they also show the reactor's capability for destroying the analytes in a single pass. Unlike the UV optimization experiments, the flow experiments studied the reactor's performance in a single-pass situation. The results demonstrate the ability of the reactor to remove between 85% and 95% of target analytes in a single pass with the longer EBCT. Importantly, both toluene and chlorobenzene were removed to 10 μg/L and 13 μg/L respectively. This is far below the USEPA National Primary Drinking Water Standards of 1000 μg/L for toluene and 100 μg/L for chlorobenzene. The USEPA does not have Primary Drinking Water Standards for the other target analytes in this study.

Figure 24 displays the data in a different manner. This graph shows the normalized removal of the contaminants with respect to the length of EBCT (empty bed contact time) in the reactor. The tendency for the reactor to quickly remove the contaminants to a certain concentration and then level off in degradation rate is clearly visible in Figure 24.

The data from Figures 23 and 24 were used to assess the reaction rate constants of the five target analytes shown in these figures. As discussed in the literature review chapter, the Langmuir-Hinshelwood (LH) equation has been shown by many researchers

to model the degradation rates in photocatalytic oxidation. The LH equation is shown in Equation 14.

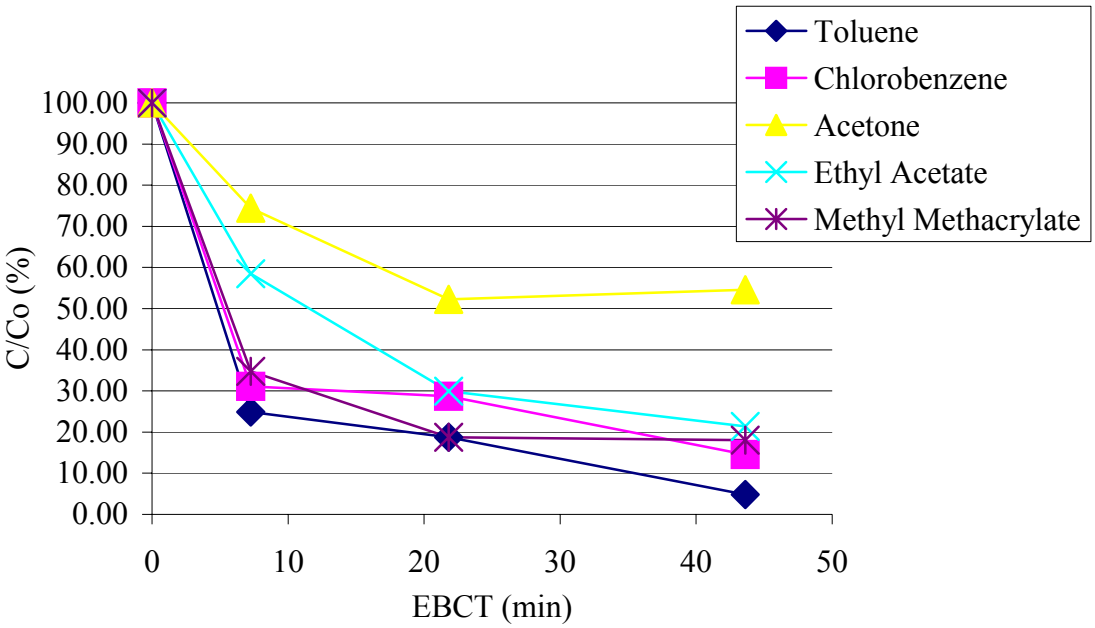

Figure 24. Degradation of five target analytes in the reactor using three UV lamps and operating the system in a single-pass mode after adsorption for five hours in a circulation mode had taken place. EBCT stands for Empty Bed Contact Time.

$$\text{rate} = kK_1C/(1+K_1C) \qquad \text{(Eq.14)}$$

where the rate is the actual rate of photocatalysis, k, is a rate constant, C is the bulk concentration of contaminant in the solution, and K_1 is an adsorption equilibrium constant based on the tendency for the contaminant to adsorb to the photocatalyst surface.

As the term K_1C becomes smaller ($1 >> K_1C$) the right hand side of Equation 14 reduces to Equation 15. Equation 15 is a simplified version of the LH equation and is recognized as a first-order rate equation.

$$\text{rate} = dC/dt = kK_1C = k'C \qquad \text{(Eq.15)}$$

where k' is used to represent the combination of the k and K_1 terms. During this research the concentrations were kept low (100 – 300 μg/L) because NASA needs to remove

contaminants that will be at this approximate concentration level. The K_1 term was not studied in this research. Therefore, it was not determinable if K_1C could be considered minimal compared to 1. However, for the ease of modeling an attempt was made to model the oxidation kinetics in the reactor using first-order kinetics. After performing the analysis, it will be shown how accurately the reactions for the contaminants behaved as approximately first order.

In the Methods chapter (Reactor hydrodynamics) it is shown that through a tracer analyses the reactor performed as 3.9 CMFRs in series. The first order equation for 1 CMFR is shown in Equation 16.

$$C/Co = (1+k\ t_{bar})^{-1} \qquad \text{(Eq.16)}$$

where C is the effluent concentration, Co is the influent concentration, k is the reaction rate constant, and t_{bar} represents the mean residence time through the reactor. To obtain the equation for 3.9 CMFRs in series, Equation 15 is used around each CMFR. By using Equation 15, the effluent to the first CMFR is found, and then the second, and this is continued until the number of CMFRs to be represented has been accomplished. A simplification to this process is Equation 17.

$$C/Co = (1 + k\ t_{bar}/n)^{-n} \qquad \text{(Eq.17)}$$

where n represents the number of CMFRs in series. In this analysis, the k' being solved for can be inserted in place of the k shown in Equation 17. This is shown in Equation 18.

$$C/Co = (1 + k'\ t_{bar}/n)^{-n} \qquad \text{(Eq.18)}$$

In order to determine k' for the target analytes in this research, it was necessary to rearrange Equation 18. Equation 18 was rearranged algebraically to form Equation 19.

$$n\ ((Co/C)^{1/n} - 1) = k'\ t_{bar} \qquad \text{(Eq.19)}$$

Equation 19 was then used to graphically determine the k' constant for each of the five compounds studied in the Effects of Empty Bed Contact Time section. This was done by graphing the left-hand side of Equation 19 on the y-axis versus t_{bar} on the x-axis. The resulting graphs, Figures 25 and 26, have trend lines with slopes equal to the k' for each specific contaminant. If the volume within the reactor were composed entirely of solution, then the slopes would represent the actual first order rate constant. The reactor, however, is composed of volume occupied by 75% solution and 25% pellets, therefore porosity must be accounted for. To do this, Equation 20 was used.

$$k_{observed} = k' / \phi \qquad \text{(Eq. 20)}$$

where $k_{observed}$ is the first order reaction rate constant found reported for this system and ϕ is the porosity of the reactor (0.75). The real first order rate constants, determined by using the slopes from Figures 25 and 26 in Equation 20, are shown in Table 5.

To assess how well a contaminant was modeled using the first order rate equation the following facts were considered. A higher R^2 (>0.8) represents a contaminant that more closely resembles a first-order reaction rate. The lower R^2 (<0.8) for acetone and methyl methacrylate suggest that a first-order reaction rate is probably not an acceptable assumption for these contaminants. Of additional importance is the intercept of the equations. Ideally, these intercepts would be zero. The presence of a y-intercept emphasizes the fact that there is a fast initial period of contaminant transformation after which the rate of removal becomes more linear with respect to EBCT.

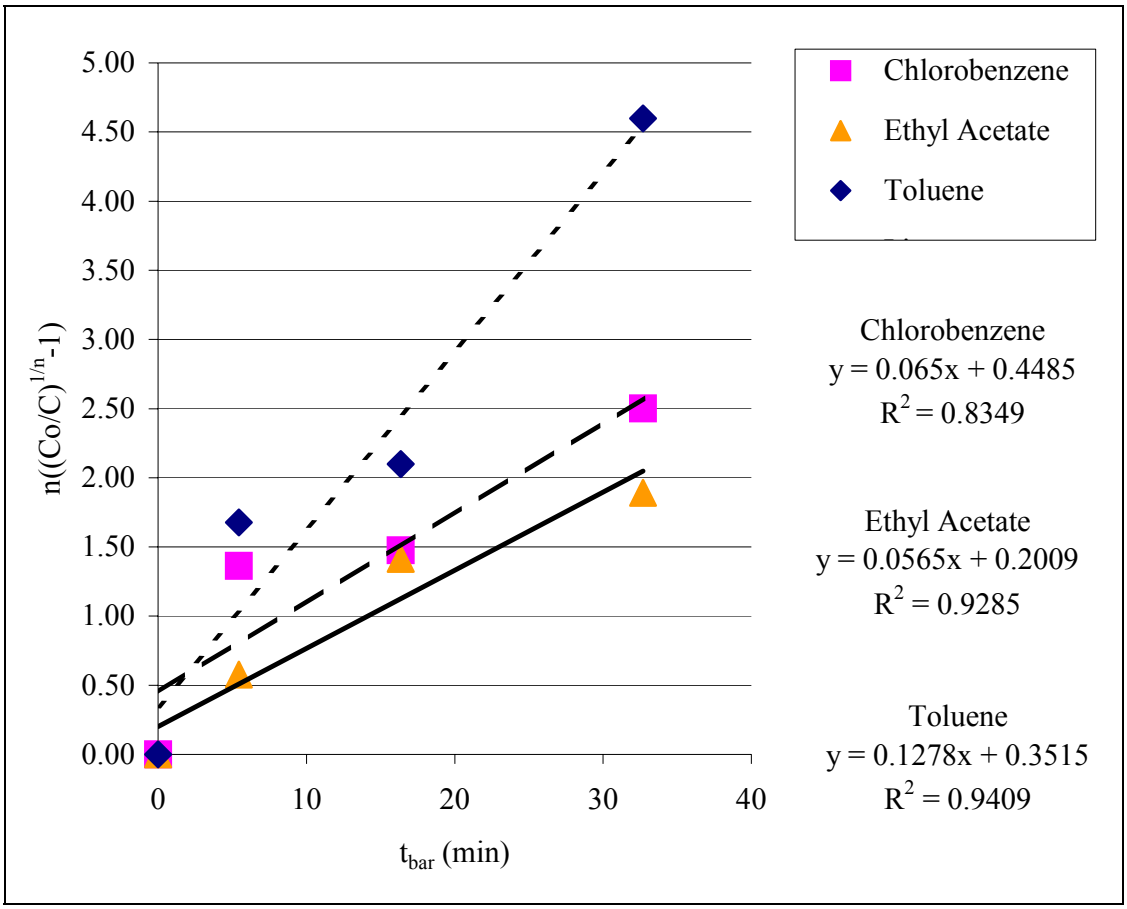

Figure 25. The slope of the trend lines produced for each target analyte represents the kinetic rate for that contaminant based on the assumption that its degradation is first-order in nature. These data are based on information from Figure 24. This figure only shows the compounds with higher R^2 values (values > 0.8).

The observed reaction rate constants predicted in Table 5 are very similar to those seen by other researchers for TiO_2 slurry. Kawaguchi (1990) reported a first order rate constant of 0.065 min^{-1} for chlorobenzene degradation at a pH of 3.5. The pH in the effluent of the reactor used in this research was approximately 3.8. In 2000, Vijayaraghavan reported a first order rate constant for toluene of 1.272 min^{-1} at a pH of 4.0. Although, the first order rate constants for each compound are similar, the form of the photocatalyst, TiO_2, is significantly different. Both of these prior researchers used TiO_2 in a slurry form in order to achieve photocatalytic oxidation. In this research similar kinetic rates were achieved in a packed bed configuration using silica gel as a support for

the TiO_2. Comparisons of these reaction rate constants are complicated by the different TiO_2 loadings, UV energy, pH, and reaction temperature, which likely were different in each case reported in the literature; however, the results show that the silica gel doped with TiO_2 was capable of degrading these target organic analytes with rates that compare well with TiO_2 slurries.

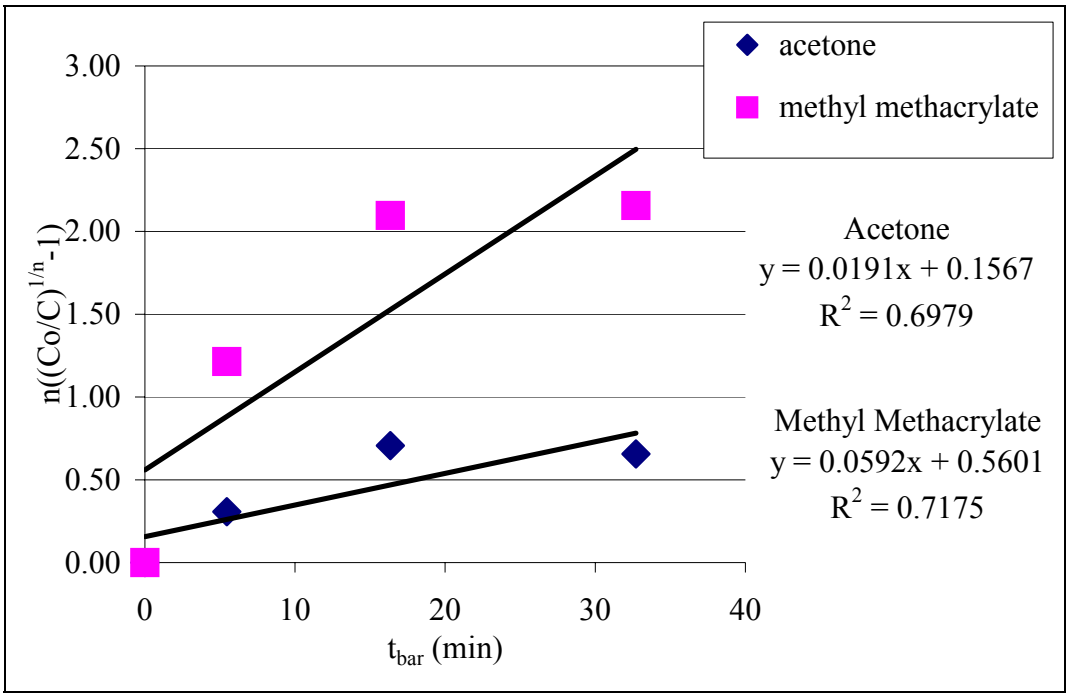

Figure 26. The slope of the trend lines produced for each target analyte represents the kinetic rate for that contaminant based on the assumption that its degradation is first-order in nature. These data are based on information from Figure 24. This figure only shows the compounds with lower R^2 values (values < 0.8).

Table 5. Important data gathered from the trend lines shown in Figures 25 and 26. The reaction rate constant (k) shown in this table is the first order rate constant for each of the listed target contaminants. These experiments were performed at a pH of 3-4 and an average temperature of approximately 25 °C.

Chemical	k (min^{-1})	R^2
Acetone	0.025	0.698
Chlorobenzene	0.086	0.835
Ethyl Acetate	0.075	0.929
Methyl Methacrylate	0.079	0.718
Toluene	0.170	0.941

Extended Duration Experiment

An experiment was performed to determine whether or not the reactor was capable of completely degrading the initial contaminant concentration to a level below detection. This experiment was performed in the same manner as the UV optimization experiments. However, samples were only taken of the initial stock solution and the final effluent concentration after 23 hours of exposure to photocatalytic oxidation. Results as shown in Table 6 demonstrate that the reactor is capable of completely removing toluene, carbon disulfide, chlorobenzene, acetone, ethyl acetate, and methyl methacrylate to concentrations that are below the detection limit of the GC/MS procedure.

Table 6. Results of the extended duration test performed for 23 hours. Initial concentrations represent the concentration of contaminant introduced to the system before any adsorption or photocatalysis took place. Final Concentrations represent the concentration of contaminant found in a sample taken after 23 hours of exposure to photocatalytic oxidation.

Chemical	Initial Concentration (μg/L)	Final Concentration (μg/L)
Acetone	321	BDL
Carbon Disulfide	220	BDL
Chlorobenzene	205	BDL
Ethyl Acetate	266	BDL
Methyl Methacrylate	319	BDL
Toluene	141	BDL

Method detection limit = 5 μg/L
Below detection limit (BDL)

Removal of Butyl Alcohol and Indole

Results from experiments performed on the degradation of butyl alcohol and indole produced data proving the reactor's capability to degrade indole and butyl alcohol with the same level of proficiency as it did the other compounds. The method for performing

these tests was previously described in the Methods section (Removal of indole and butyl alcohol).

Figure 27 shows the results of the degradation experiments performed with the system operating in a circulation mode. The contaminants in these experiments experienced 5 hours of adsorption in the system and then 6 hours of photocatalytic oxidation. Figure 28 shows the degradation results from a single pass through the reactor. The EBCTs for the experiments shown in Figure 28 were 43.6 minutes.

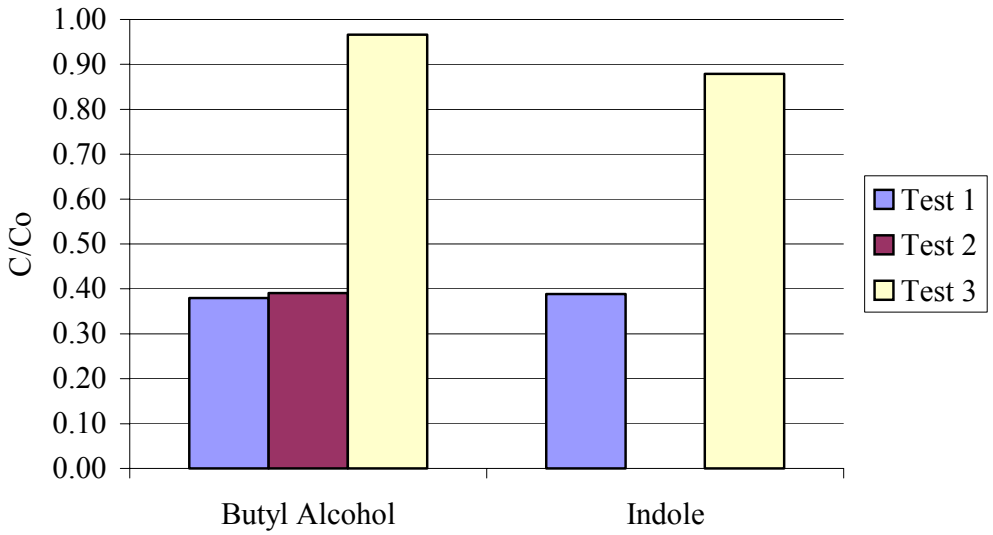

Figure 27. Results showing the degradation of butyl alcohol and indole as a result of 6 hours of exposure to UV radiation. A 4-liter source tank was used in this reactor system. There appears to be no data for the indole in the second test because the data point is 0.

With the exception of the 3rd experiment (it is believed that there may be some error in this experiment), the data demonstrate excellent removal of both butyl alcohol and indole. The 2nd experiment, in fact, showed destruction of indole to beyond the detection level. The 4th and 5th experiments were especially promising, because they show 93 to 97% removal of both butyl alcohol and indole in a single pass through the reactor. The rapid removal of butyl alcohol and indole is particularly important since it

has been stated in literature that their removal should be a greater challenge to the reactor than the removal of the other 6 analytes (Serpone, 1995).

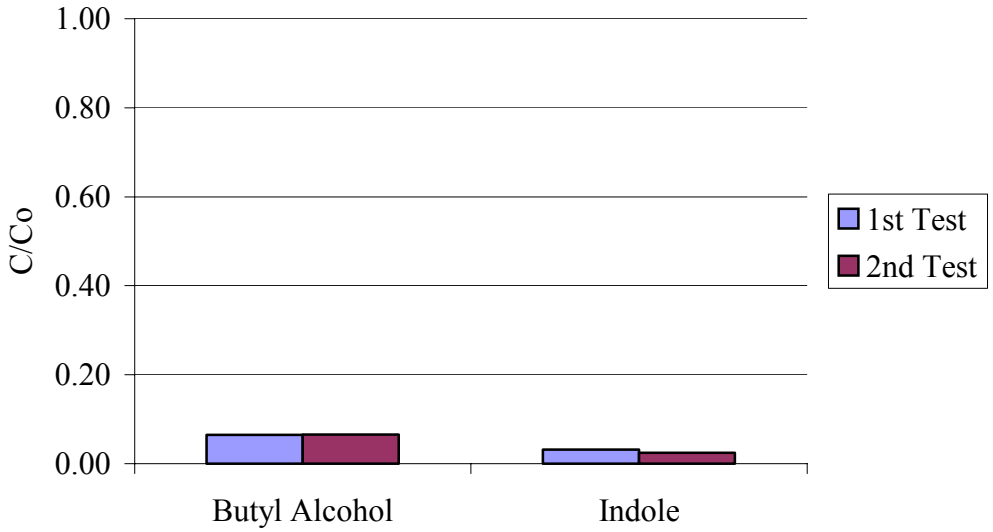

Figure 28. Data showing the ratio of each chemical's concentration in the sample from Port 2 versus the sample from Port 1.

CHAPTER 5
SUMMARY AND CONCLUSIONS

Summary

Eight target analytes including acetone, butyl alcohol, carbon disulfide, chlorobenzene, ethyl acetate, indole, methyl methacrylate, and toluene, were tested for their degradation using the process of photocatalytic oxidation. The photocatalytic oxidation was carried out in an annular reactor with the TiO_2 supported on a silica gel matrix and arranged in a packed bed style within the reactor. Adsorption and desorption of the contaminants within the reactor were studied to determine the capabilities of the photocatalyst pellets for removing contaminants without photocatalytic oxidation. The level of available electron acceptor (in the form of DO) and the effects of UV radiation intensity were studied to investigate their impact on the process. Ability of the reactor to remove all of the target analytes was assessed. Finally, the reactor was tested for its removal of 5 target analytes at various EBCTs. Results of those experiments were used to determine rates of photocatalytic oxidation within the reactor.

Conclusions

An annular reactor containing silica/titania pellets arranged in a packed bed style is capable of degrading all 8 of this research's target analytes. Six of the compounds were degraded to below detection limit (5 μg/L) after an extended reaction period. Photocatalytic destruction of the contaminants in the reactor was not limited by UV radiation intensity beyond the use of 1 lamp (8 Watts), providing approximately 4.44 W of energy to the interior surface of the reactor. Photocatalysis was also not limited by the

amount of oxygen when the dissolved oxygen level was 5.4 mg/L; however, lower levels of dissolved oxygen were not investigated. A possibility does exist that adsorption of contaminants to the pellet surface will occur if a proper gradient exists between the concentration in aqueous solution and the concentration attached to the surface of the pellets. That sorption was also found to be reversible. First order rate constants for the photocatalytic degradation of both toluene and chlorobenzene were similar to those reported for TiO_2 photocatalysis in slurry form. One possible reason for this is the loading. Loading rates for this research were approximately 87 g of TiO_2/L of solution (some of that is certainly trapped within the pellets). Loading rates for one of the slurry experiments was only 1 g of TiO_2/L of solution. In spite of the fast degradation rates, EBCT does play a part in the level of degradation seen in the effluent. Once exact concentrations and flow rates are known by NASA it will be important to find an exact EBCT necessary to achieve proper degradation.

This research has proven the hypothesis by showing the potential for titania/silica pellets arranged in a packed-bed-style reactor to significantly degrade 8 organic compounds in a mixed solution. This research must be taken to further levels by including it within a treatment process train, using actual wastewater or simulated wastewater formulations and assessing its ability at practical flow rates and over longer periods of time.

APPENDIX A
CHEMICAL INFORMATION

Table 7. Table of Target Analytes

Analytes	Formula	Volume of Sample (mL)	Container	Method #	Sample Preservation	Holding Time
Chlorobenzene	C_6H_5Cl	40	VOA vial with Teflon seals	USEPA 524.2	4 degrees Celsius	2 weeks
Acetone	C_3H_5O	40	VOA vial with Teflon seals	USEPA 524.2	4 degrees Celsius	2 weeks
Indole	C_8H_7N	40	VOA vial with Teflon seals	SPME	4 degrees Celsius	2 weeks
Butyl Alcohol	$C_4H_{10}O$	40	VOA vial with Teflon seals	SPME	4 degrees Celsius	2 weeks
Toluene	C_7H_8	40	VOA vial with Teflon seals	USEPA 524.2	4 degrees Celsius	2 weeks
Ethyl Acetate	$C_4H_8O_2$	40	VOA vial with Teflon seals	USEPA 524.2	4 degrees Celsius	2 weeks
Methyl Methacrylate	$C_5H_8O_2$	40	VOA vial with Teflon seals	USEPA 524.2	4 degrees Celsius	2 weeks
Carbon Disulfide	CS_2	40	VOA vial with Teflon seals	USEPA 524.2	4 degrees Celsius	2 weeks

Table 8. Molecular Weight of Target Analytes

Compound	Molecular Weight (amu)
Acetone	57.072
Butyl Alcohol	74.122
Carbon Disulfide	76.131
Ethyl Acetate	88.105
Toluene	92.14
Methyl Methacrylate	100.116
Chlorobenzene	112.559
Indole	117.15

Table 9. Henry's Constants and Partitioning Coefficients

Chemical	Henry's Constant (atm/mol fraction)	Log of the Partitioning Coefficient (octanol-water coeff.)
butanol	0.7	0.88
acetone	1.4	-0.24
ethyl acetate	7.7	0.73
methyl methacrylate	7.8	1.38
chlorobenzene	209.0	2.92
toluene	356.7	2.69
carbon disulfide	1064.0	2.14
indole	10739.0	2.14

(Yaws, 1999; The Federal Register; http://www.ccc.uni-erlangen.de; Schwarzenbach, 1993)

Table 10. Melting Points/Boiling Points

Chemical	Melting Point ^{o}C	Boiling Point ^{o}C
acetone	-95	56.2
butyl alcohol	-89.9	117.7
carbon disulfide	-108.6	46.3
chlorobenzene	-45	132
ethyl acetate	-83.6	77
indole	52.5	254
methyl methacrylate	-50	101
toluene	-95.1	110.8

Table 11. Sources of Contaminant

Chemical	Source
Acetone	Varnishes, adhesives, and humans.
Butyl Alcohol	Gasoline.
Carbon Disulfide	Rubber chemicals.
Chlorobenzene	Dyes and insectisides.
Ethyl Acetate	Solvents and adhesives
Indole	Humans.
Methyl Methacrylate	Plastics.
Toluene	rubbers.

(Verschueren, 1983; http://www.epa.gov; http://www.echeminc.com)

Table 12. Contaminant Generation in the ALS

Chemical	Equipment Genereration Rate (mg/day*kg)	Metabolic Generation Rate (mg/man*day)
Acetone	3.62E-03	2.00E-01
Butyl Alcohol	4.71E-03	1.33E+00
Carbon Disulfide	3.23E-05	0.00E+00
Chlorobenzene	1.54E-03	0.00E+00
Ethyl Acetate	2.97E-04	0.00E+00
Indole	0.00E+00	6.25E+00
Methyl Methacrylate	1.30E-04	0.00E+00
Toluene	1.98E-03	0.00E+00

(Lange, 1998)

Table 13. Water Quality Requirements

Parameter	Potable Water Specifications	Hygiene Specifications
Total Solids	100 mg/L	500 mg/L
pH	6.0 - 8.5	5.0 - 8.5
Turbidity	1.0 NTU	1.0 NTU
Cations	30 mg/L	N/A
Anions	30 mg/L	N/A
CO_2	15 mg/L	N/A
Total Acids	500 mg/L *	500 mg/L *
TOC	500 mg/L *	10,000 mg/L *
Halogenated Hydrocarbons	10 mg/L *	10 mg/L *
Total Phenols	1 mg/L *	1 mg/L *
Total Alcohols	500 mg/L *	500 mg/L *
Cyanide	200 mg/L *	200 mg/L *

* Although the source reports these units as mg/L it seems probable that it should actually be reported as μg/L.

(Lange, 1998)

Table 14. Spacecraft Trace Contaminant Generation Rates

COMMON NAME	MOLAR MASS g/mol	SMAC mg/m3	EQUIPMENT GEN RATE mg/day*kg	METABOLIC GEN RATE mg/man*day
ALCOHOLS				
Methyl alcohol	32.04	9	1.27E–03	1.50E+00
Ethyl alcohol	46.07	94	7.85E–03	4.00E+00
Allyl alcohol	58.08	1	2.35E–06	0.00E+00
Isopropyl alcohol	60.09	150	3.99E–03	0.00E+00
Propyl alcohol	60.09	98.3	2.41E–04	0.00E+00
Ethylene glycol	62.07	127	6.03E–06	0.00E+00
2–butanol	74.12	121	9.63E–06	0.00E+00
Isobutyl alcohol	74.12	121	8.46E–04	1.20E+00
tert–butyl alcohol	74.12	121	7.38E–05	0.00E+00
Butyl alcohol	74.12	121	4.71E–03	1.33E+00
n–amyl alcohol	88.15	126	1.62E–04	0.00E+00
Phenol	94.11	7.7	4.83E–04	0.00E+00
Hexahydrophenol	100.16	123	7.56E–04	0.00E+00
2–hexanol	102.18	167	2.48E–06	0.00E+00

Table 14 (continued)

ALDEHYDES				
Formaldehyde	30.03	0.05	4.40E–08	0.00E+00
Acetaldehyde	44.05	4	1.09E–04	9.00E–02
Acrolein	56.06	0.03	3.46E–06	0.00E+00
Propionaldehyde	58.08	95	3.19E–04	0.00E+00
n–butylaldehyde	72.1	118	8.59E–04	0.00E+00
valeraldehyde	86.13	106	7.84E–05	8.30E–01
benzenecarbonal	106.12	173	1.99E–05	0.00E+00
AROMATIC HYDROCARBONS				
Benzene	78.11	0.32	2.51E–05	0.00E+00
Toluene	98.13	60	1.98E–03	0.00E+00
Styrene	104.14	42.6	3.13E–05	0.00E+00
o–xylene	106.16	86.8	5.56E–04	0.00E+00
m–xylene	106.16	86.8	2.03E–03	0.00E+00
p–xylene	106.16	86.8	1.08E–03	0.00E+00
Ethylbenzene	106.16	86.8	1.50E–04	0.00E+00
alpha–methylstyrene	118.18	145	1.67E–07	0.00E+00
Pseudocumene	120.2	15	4.49E–05	0.00E+00
Mesitylene	120.2	15	3.63E–06	0.00E+00
1–ethyl–2–methylbenzene	120.2	25	4.88E–06	0.00E+00
Cumene	120.2	73.7	1.40E–05	0.00E+00
Propylbenzene	120.2	49.1	2.15E–04	0.00E+00
ESTERS				
ethyl formate	74.08	90.9	4.51E–06	0.00E+00
methyl acetate	74.08	121	1.41E–04	0.00E+00
ethyl acetate	88.11	180	2.97E–04	0.00E+00
methyl methacrylate	100.12	102	1.30E–04	0.00E+00
isopropyl acetate	102.13	209	5.81E–06	0.00E+00
propyl acetate	102.13	167	3.38E–04	0.00E+00
butyl acetate	116.16	190	7.46E–04	0.00E+00
isobutyl acetate	116.16	190	1.52E–04	0.00E+00
ethyl lactate	118.13	193	3.64E–06	0.00E+00
n–amyl acetate	130.18	160	4.78E–05	0.00E+00
cellosolve acetate	132.16	162	7.46E–04	0.00E+00

Table 14 (continued)

ETHERS				
Furan	68.07	0.11	1.84E–06	0.00E+00
Tetrahydrofuran	72.11	118	6.93E–05	0.00E+00
Ether	74.12	242	8.90E–05	0.00E+00
sylvan	82.1	0.13	3.46E–06	0.00E+00
ethyl cellosolve	90.12	0.3	6.01E–04	0.00E+00
CHLOROCARBONS				
Methyl chloride	50.49	41.3	6.76E–06	0.00E+00
Vinyl chloride	62.5	0.26	1.46E–06	0.00E+00
Ethyl chloride	64.52	263.7	8.99E–08	0.00E+00
Methylene chloride	84.93	10	2.15E–03	0.00E+00
dichloroethene	96.95	7.9	5.64E–07	0.00E+00
Ethylene dichloride	98.97	1	7.74E–05	0.00E+00
Chlorobenzene	112.56	46	1.54E–03	0.00E+00
propylene chloride	112.99	42.2	7.42E–06	0.00E+00
Chloroform	119.38	4.9	1.76E–05	0.00E+00
Trichloroethylene	131.39	10	8.62E–05	0.00E+00
Methyl chloroform	133.41	164	6.72E–04	0.00E+00
Vinyl trichloride	133.41	5.5	8.24E–08	0.00E+00
dichorobenzene	147.01	30	6.33E–06	0.00E+00
Carbon tetrachloride	153.82	13	9.60E–06	0.00E+00
Tetrachloroethylene	165.83	34	7.28E–04	0.00E+00
CHLOROFLUOROCARBONS				
Freon 22	86.47	353.6	5.75E–05	0.00E+00
Freon 21	102.9	21	6.36E–07	0.00E+00
chlorotrifluoroethane	118.5	484.5	4.88E–06	0.00E+00
Freon 12	120.91	494.4	1.35E–05	0.00E+00
dichorodifluoroethene	132.93	136	1.89E–06	0.00E+00
Freon 11	137.4	561.8	1.41E–03	0.00E+00
Halon 1301	148.9	608.8	2.61E–04	0.00E+00
Freon 114	170.92	702.9	2.62E–05	0.00E+00
Freon 113	187.4	400	1.89E–02	0.00E+00
Freon 112	204	834.2	3.33E–05	0.00E+00

Table 14 (continued)

HYDROCARBONS				
Methane	16.04	3800	6.39E–04	1.60E+02
Ethylene	28.05	344.1	2.27E–07	0.00E+00
Ethane	30.07	1230	1.17E–06	0.00E+00
Propylene	42.08	860.3	2.56E–06	0.00E+00
Propane	44.09	901.4	9.21E–07	0.00E+00
Vinylethylene	54.09	221.2	2.66E–06	0.00E+00
Ethylethylene	56.1	458	8.03E–05	0.00E+00
Isobutane	58.12	237.6	1.10E–05	0.00E+00
Butane	58.12	237.6	5.13E–06	0.00E+00
Propylethylene	70.13	186	2.20E–08	0.00E+00
Isopentane	72.15	295	1.80E–06	0.00E+00
Pentane	72.15	590	9.54E–05	0.00E+00
hexamethylene	84.16	206	3.79E–04	0.00E+00
methylpentamethylene	84.16	51.6	2.97E–05	0.00E+00
Neohexane	86.17	88.1	1.67E–06	0.00E+00
Diethylmethylmethane	86.18	1762	5.97E–06	0.00E+00
Hexane	86.18	176	6.95E–05	0.00E+00
1–heptylene	98.18	201	1.10E–08	0.00E+00
Hexahydrotoluene	98.18	60.2	6.09E–05	0.00E+00
Heptane	100.21	205	5.59E–05	0.00E+00
Dimethylcyclohexane	112.22	115	2.61E–05	0.00E+00
trans–1,2–dimethylhexamethylene	112.22	115	5.23E–05	0.00E+00
octane	114.23	350	1.61E–05	0.00E+00
nonane	128.26	315	7.35E–06	0.00E+00
citrene (limonene)	136.23	557	3.58E–06	0.00E+00
Decane	142.28	223	2.78E–05	0.00E+00
Hendecane	156.31	319	2.51E–05	0.00E+00
Dodecane	170.34	278	6.91E–07	0.00E+00

Table 14 (continued)

KETONES				
Acetone	58.08	712.5	3.62E–03	2.00E–01
Methyl ethyl ketone	72.11	30	6.01E–03	0.00E+00
Methyl propyl ketone	86.13	70.4	4.03E–06	0.00E+00
Methyl isopropyl ketone	86.13	70.4	3.11E–05	0.00E+00
Mesityl oxide (methyl isobutenyl ketone)	98.14	40.1	1.91E–04	0.00E+00
cyclohexanone (pimelic ketone)	98.14	60.2	6.62E–04	0.00E+00
Methyl isobutyl ketone	100.16	82	1.41E–03	0.00E+00
Phenyl methyl ketone	120.14	245	5.66E–07	0.00E+00
Methyl hexyl ketone	128.21	105	1.65E–07	0.00E+00
Diisobutyl ketone	142.2	58.1	3.34E–06	0.00E+00
MERCAPTANS and SULFIDES				
hydrogen sulfide	34.08	2.8	0.00E+00	9.00E–02
Carbon oxisulfide	60.07	12	6.05E–06	0.00E+00
Methyl sulfide	62.14	2.5	1.88E–07	0.00E+00
carbon disulfide	76.14	16	3.23E–05	0.00E+00
ORGANIC ACIDS				
Acetic acid	60.05	7.4	1.42E–06	0.00E+00
ORGANIC NITROGENS				
Acetonitrile	41.05	6.7	1.70E–08	0.00E+00
Indole	117.15	0.25	0.00E+00	6.25E+00
MISCELLANEOUS				
hydrogen	2.02	340	5.91E–06	2.60E+01
ammonia	17	7	8.46E–05	3.21E+02
carbon monoxide	28.01	10	2.03E–03	2.30E+01
trimethylsilanol	90.21	40	1.69E–04	0.00E+00
hexamethylcyclotrioxosilane	222.4	227	1.62E–04	0.00E+00
octamethyltrioxosilane	236.54	40	2.11E–04	0.00E+00

(Lange, 1998)

Table 15. Spacecraft Maximum Allowable Concentrations

		Potential Exposure Period				
Chemical		1 h	24 h	7 d	30 d	180 d
ACETALDEHYDE	mg/m^3	20	10	4	4	4
ACROLEIN	mg/m^3	0.2	0.08	0.03	0.03	0.03
AMMONIA	mg/m^3	20	14	7	7	7
CARBON DIOXIDE	mm Hg	10	10	5.3	5.3	5.3
CARBON MONOXIDE	mg/m^3	60	20	10	10	10
1,2–DICHLOROETHANE	mg/m^3	2	2	2	2	1
2–ETHOXYETHANOL	mg/m^3	40	40	3	2	0.3
FORMALDEHYDE	mg/m^3	0.5	0.12	0.05	0.05	0.05
FREON 113	mg/m^3	400	400	400	400	400
HYDRAZINE	mg/m^3	5	0.4	0.05	0.03	0.005
HYDROGEN	mg/m^3	340	340	340	340	340
INDOLE	mg/m^3	5	1.5	0.25	0.25	0.25
MERCURY	mg/m^3	0.1	0.02	0.01	0.01	0.01
METHANE	mg/m^3	3800	3800	3800	3800	3800
METHANOL	mg/m^3	40	13	9	9	9
METHYL ETHYL KETONE	mg/m^3	150	150	30	30	30
METHYL HYDRAZINE	mg/m^3	0.004	0.004	0.004	0.004	0.004
DICHLOROMETHANE	mg/m^3	350	120	50	20	10
OCTAMETHYLTRISILOXANE	mg/m^3	4000	2000	1000	200	40
2–PROPANOL	mg/m^3	1000	240	150	150	150
TOLUENE	mg/m^3	60	60	60	60	60
TRICHLOROETHYLENE	mg/m^3	270	60	50	20	10
TRIMETHYLSILANOL	mg/m^3	600	70	40	40	40
XYLENE	mg/m^3	430	220	220	220	220

(Lange, 1998)

APPENDIX B
REACTOR INFORMATION

Table 16. Predicted Retention Time Calculations

Cylindrical Reactor:

Length of Reactor =	14.0 cm
Inner Diameter =	8.5 cm
Width of Space =	1.0 cm
Outer Diameter =	10.5 cm

Volume = 418 cm^3 = 418 mL

Cyllindrical Reactor:

Actual Volume with ends is 436 mL.

Volume available for polluted waters is 436*.75

Volume = 327 mL

Flow through the reactor is approximated as:

(167.8kgH_2O/day/6persons)*(6persons)*(1000g/kg)*(cm^3/g)*
(mL/cm3)*(day/24hrs)*(hr/60min)

Flow = 116.5 mL H2O/min

Flow through the reactor during testing will be:

Flow = 10 mL H20/min

The retention time with the ALS flow is about 327 / 116.5 =

Time = 2.81 min

The retention during testing is about 327 / 10 =

Time = 32.7 min

Table 17. System Volume Calculation

Component			Volume for Water
Reactor:		=	327 mL
Tubing:			
	6 mm OD Tubing	=	4.071 mL
	1/4 inch ID tubing	=	156 mL
Source Tank:		=	1000 mL or 4000 mL
System Volume with 1L source tank:		=	1487 mL or 1.49 L
System Volume with 4L source tank:		=	4487 mL 4.49 L

Table 18. KCl Conductivities for Testing Probe Accuracy

KCl equivalent/L	Equivalent Conductivity, L mho-cm2/equivalent	Conductivity, k mmho/cm
0	149.9	
0.0001	148.9	14.9
0.0005	147.7	73.9
0.001	146.9	146.9
0.005	143.6	717.5
0.01	141.2	1412
0.02	138.2	2765
0.05	133.3	6667
0.1	128.9	12890
0.2	124.0	24800
0.5	117.3	58670
1	111.9	111900

(Standard Methods, 1998)

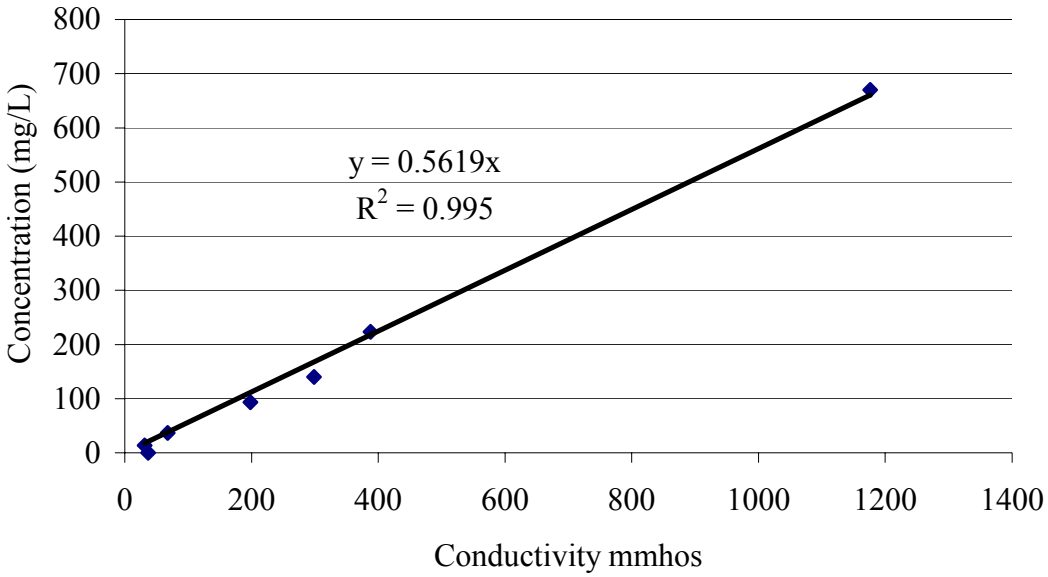

Figure 29. Concentration of NaCl in deionized water solution versus the conductivity read on a Fisher Scientific conductivity probe.

Table 19. Calculation of Flow Regime in the Reactor

$N_{RE} = (d_m * V_o * r_L) / (m*(1-e_o))$

d_m = Diameter of the media =	3	mm
V_o = Velocity of the liquid =	Q/A	
A = Cross sectional are of the reactor =	29.85	cm^2
r_L = Density of the liquid =	998.2	kg/m^3
m = Viscosity of the liquid =	0.001002	$N*s/m^2$
e = Interparticular porosity of the media =	0.75	

	N_{RE}	Q (mL/min)
Testing Flows	0.67	10
	1.33	20
	4.00	60
NASA predicted flow	7.78	116.5

$N_{RE} < 10$ is in the laminar regime.

Table 20. Calculation of UV Energy at Reactor Surface

UV Intensity Calculations	
2.06 mW/cm^2	<= UV measured at reactor end
21.7 mW/cm^2	<= UV measured at reactor center
2.06 mW/cm^2	<= UV measured at reactor end
11.88 mW/cm^2	<= Average intensity from beginning to middl
11.88 mW/cm^2	<= Average intensity from middle to end
374 cm^2	<= Reactor's inner surface area
187 cm^2	<= Reactor's area from beginning to middle
187 cm^2	<= Reactor's area from middle to end
2221.56 mW	<= Energy to reactor from beginning to middle
2221.56 mW	<= Energy to reactor from middle to end
4443.12 mW	<= Total energy to reactor

APPENDIX C
RAW DATA

Table 21. Initial Raw Data Test (1/6/3)

Chemical	RF (AVG)	%RSD	Stock Solution (μg/L)	t = 0 (μg/L)	t = 118 (μg/L)	t = 238 (μg/L)	t = 349 (μg/L)
Carbon Disulfide	0.9448	20.26	94.1	33.2	15.5	4.8	3.0
Chlorobenzene	1.1648	25.14	67.7	34.2	15.0	5.6	3.0
Toluene	3.176	30.03	64.8	45.1	19.3	6.8	3.8

Table 22. Volatility Test Raw Data (2/6/3)

Chemical	RF (AVG)	%RSD	Stock Solution (μg/L)	t = 120 (μg/L)	t = 240 (μg/L)	t = 360 (μg/L)	t = 480 (μg/L)
Chlorobenzene	2.46	34	126.6	122.8	109.1	86.9	103.9
Toluene	4.39	35	56.1	55.1	48.6	33.8	47.2

Table 23. Adsorption Test Raw Data (3/8/3)

Chemical	RF (AVG)	%RSD	Stock Solution (μg/L)	t = 60 (μg/L)	t = 120 (μg/L)	t = 235 (μg/L)	t = 295 (μg/L)
Chlorobenzene	2.24	9.7	120.6	104.8	78.4	71.6	66.2
Toluene	4.47	15.2	75.6	67.9	52.4	50.9	46.9

Table 24. UV Optimization (3 Lamps) Raw Data (3/12/3)

Chemical	RF (AVG)	%RSD	Stock Solution (μg/L)	t = 0 (μg/L)	t = 120 (μg/L)	t = 240 (μg/L)	t = 360 (μg/L)
Carbon Disulfide	1.29	14.6	122.7	50.0	34.4	14.7	6.3
Chlorobenzene	2.24	9.7	153.4	74.5	48.5	20.3	9.1
Ethyl Acetate	0.10	0	19.2	13.0	10.0	4.6	1.8
Methyl Methacrylate	0.059	8.19	139.0	82.2	49.3	17.2	4.5
Toluene	4.05	15.2	102.4	56.6	37.3	18	11

Table 25. UV Optimization (2 Lamps) Raw Data (3/13/3)

Chemical	RF (AVG)	%RSD	t = 0 (µg/L)	t = 240 (µg/L)	t = 360 (µg/L)
Carbon Disulfide	1.29	14.6	60.7	20.5	9.4
Chlorobenzene	2.24	9.7	69.0	22.6	9.1
Ethyl Acetate	0.10	0	84.2	13.6	13.9
Methyl Methacrylate	0.059	8.19	73.3	19.6	6.0
Toluene	4.05	15.2	62.0	22.6	12.7

Table 26. UV Optimization (1 Lamp) Raw Data (3/14/3)

Chemical	RF (AVG)	%RSD	t = 0 (µg/L)	t = 120 (µg/L)	t = 246 (µg/L)	t = 360 (µg/L)
Carbon Disulfide	1.14	25.7	60.6	25.2	12.5	6.7
Chlorobenzene	2.51	15.1	74.7	47.5	22	10.9
Ethyl Acetate	0.02	0	50.4	35.5	19.6	11.6
Methyl Methacrylate	0.0594	8.8	124.4	64.3	27.9	14.8
Toluene	6.07	38.5	44.3	26.8	11.6	5.2

Table 27. UV Optimization (2 Lamp Duplicate) Raw Data (3/17/3)

Chemical	RF (AVG)	%RSD	t = 0 (µg/L)	t = 120 (µg/L)	t = 240 (µg/L)	t = 360 (µg/L)
Carbon Disulfide	1.14	25.7	47.6	25.5	18.2	10.7
Chlorobenzene	2.51	15.1	54.3	33.8	18.6	10.4
Ethyl Acetate	0.02	0	43.4	34.1	19.9	10.1
Methyl Methacrylate	0.0594	8.8	94.7	56.6	28.4	12.4
Toluene	6.07	38.5	55.0	32.1	16.6	8.4

Table 28. 11-Hour Adsorption Experiment Raw Data (4/3/3)

Chemical	RF (AVG)	%RSD	t = 0 (μg/L)	t = 0 (dup) (μg/L)
Carbon Disulfide	1.02	13.8	54.4	46.0
Chlorobenzene	3.05	15.3	150.5	158.7
Ethyl Acetate	0.02	0	120.1	119.3
Methyl Methacrylate	0.076	10.2	213.0	221.2
Toluene	7.29	38.4	111.5	118.0

t = 75 (μg/L)	t = 255 (μg/L)	t = 375 (μg/L)	t = 555 (μg/L)	t = 735 (μg/L)
33.0	24.8	24.8	21.5	16.0
88.6	67.3	67.3	61.6	53.1
66.2	52.6	52.6	47.2	37.2
125.3	102.7	102.7	97.2	82.3
72.4	59.9	59.9	57.1	50.2

Table 29. 60 mL/min Flow Test (Series 2) Raw Data (4/6/3)

Chemical	RF (AVG)	%RSD	Stock (μg/L)	t = 3.5 (μg/L)	t = 5 (μg/L)	Port 1 (μg/L)	Port 2 (μg/L)
Acetone	0.02	30.6	159.7	105.2	75.3	109.0	37.9
Carbon Disulfide	2.49	25.4	186.8	87.1	82.3	44.3	4.7
Chlorobenzene	2.70	21.3	1080.9	572.6	527.4	313.1	77.7
Ethyl Acetate	0.25	20.1	5.1	3.4	4.5	2.7	0.9
Methyl Methacrylate	0.04	8.3	116.8	73.5	70.1	51.1	10.0
Toluene	7.84	40.1	42.2	29.0	29.0	15.3	2.6

*Port 1 is before the reactor *Port 2 is after the reactor

Table 30. 20 mL/min Flow Test (Series 2) Raw Data (4/9/3)

Chemical	RF (AVG)	%RSD	Stock (µg/L)	t = 3.5 (µg/L)	t = 5 (µg/L)	Port 1 (µg/L)	Port 2 (µg/L)
Acetone	0.02	30.6	11.8	66.3	45.2	42.0	36.6
Carbon Disulfide	2.49	25.4	128.7	79.8	85.4	54.3	20.3
Chlorobenzene	2.70	21.3	133.3	61.1	77.3	60.9	18.5
Ethyl Acetate	0.25	20.1	10.8	7.4	7.6	6.5	3.9
Methyl Methacrylate	0.04	8.3	290.7	189.5	175.8	152.5	61.6
Toluene	7.84	40.1	117.9	54.1	72.9	53.4	11.9

*Port 1 is before the reactor *Port 2 is after the reactor

Table 31. 10 mL/min Flow Test (Series 2) Raw Data (4/7/3)

Chemical	RF (AVG)	%RSD	Stock (µg/L)	t = 3.5 (µg/L)	t = 5 (µg/L)	Port 1 (µg/L)	Port 2 (µg/L)
Acetone	0.02	30.6	144.0	90.2	94.9	127.6	95.2
Carbon Disulfide	2.49	25.4	36.5	27.6	25.1	22.7	13.9
Chlorobenzene	2.70	21.3	288.8	108.7	118.4	95.0	13.8
Ethyl Acetate	0.25	20.1	10.6	6.7	6.8	6.4	1.8
Methyl Methacrylate	0.04	8.3	355.9	210.6	179.2	168.0	43.8
Toluene	7.84	40.1	107.3	43.2	43.2	44.3	0.9

*Port 1 is before the reactor *Port 2 is after the reactor

Table 32. 23-Hour Test Raw Data (4/16/3)

Chemical	RF (AVG)	%RSD	Stock (µg/L)	Stock (dup) (µg/L)	t = 23 hours (µg/L)	t = 23 hours (dup) (µg/L)
Acetone	0.02	20.3	263.4	379.2	3.7	2.3
Carbon Disulfide	1.96	14.9	225.2	214.3	5.9	4.0
Chlorobenzene	2.60	3.2	194.1	216.7	3.6	4.3
Ethyl Acetate	0.01	0.0	263.8	267.2	0.0	0.0
Methyl Methacrylate	0.04	10.7	295.6	342.4	0.0	0.0
Toluene	5.32	4.2	138.9	142.7	1.7	1.8

*Port 1 is before the reactor *Port 2 is after the reactor

Table 33. 60 mL/min Flow Test (Series 3) Raw Data (4/28/3)

Chemical	RF (AVG)	%RSD	Stock (µg/L)	t = 3.5 (µg/L)	t = 5 (µg/L)	Port 1 (µg/L)	Port 2 (µg/L)
Acetone	0.02	20.3	270.1	293.0	304.4	314.5	194.3
Carbon Disulfide	1.96	14.9	2.2	1.6	1.1	0.8	0.2
Chlorobenzene	2.60	3.2	191.3	167.3	135.8	151.4	48.4
Ethyl Acetate	0.01	0.0	213.1	200.1	167.6	189.7	107.2
Methyl Methacrylate	0.04	10.7	8.5	7.7	6.7	7.3	2.1
Toluene	5.32	4.2	118.1	107.2	91.1	95.5	26.1

*Port 1 is before the reactor *Port 2 is after the reactor

Table 34. 20 mL/min Flow Test (Series 3) Raw Data (4/25/3)

Chemical	RF (AVG)	%RSD	Stock (µg/L)	t = 3.5 (µg/L)	t = 5 (µg/L)	Port 1 (µg/L)	Port 2 (µg/L)
Acetone	0.02	20.3	609.0	520.9	356.8	427.1	297.8
Carbon Disulfide	1.96	14.9	11.0	5.3	7.5	22.7	16.8
Chlorobenzene	2.60	3.2	236.1	241.3	194.8	89.5	29.1
Ethyl Acetate	0.01	0.0	253.8	229.0	205.7	186.2	51.5
Methyl Methacrylate	0.04	10.7	41.4	38.1	32.5	25.9	4.6
Toluene	5.32	4.2	140.7	136.9	113.3	27.6	11.7

*Port 1 is before the reactor *Port 2 is after the reactor

Table 35. 10 mL/min Flow Test (Series 3) Raw Data (4/27/3)

Chemical	RF (AVG)	%RSD	Stock (µg/L)	t = 3.5 (µg/L)	t = 5 (µg/L)	Port 1 (µg/L)	Port 2 (µg/L)
Acetone	0.02	20.3	609.6	408.0	259.9	474.0	163.7
Carbon Disulfide	1.96	14.9	0.5	2.0	1.9	1.9	0.5
Chlorobenzene	2.60	3.2	103.2	99.2	82.1	87.2	12.7
Ethyl Acetate	0.01	0.0	148.9	129.1	120.0	127.0	19.6
Methyl Methacrylate	0.04	10.7	10.3	9.5	8.2	8.5	0.8
Toluene	5.32	4.2	166.4	135.0	110.6	129.7	10.0

*Port 1 is before the reactor *Port 2 is after the reactor

Table 36. 1st Desorption Test Raw Data (5/13/3)

Chemical	RF (AVG)	%RSD	t = 0 (µg/L)	t = 5 (µg/L)
Acetone	0.02	60.0	184.9	104.0
Carbon Disulfide	2.20	34.1	194.5	83.4
Chlorobenzene	2.57	17.5	217.7	231.2
Ethyl Acetate	0.22	20.0	10.9	12.7
Methyl Methacrylate	0.05	17.8	376.1	328.4
Toluene	5.26	18.8	190.3	119.2

Rinse (µg/L)	Rinse (DUP) (µg/L)	45 min Desorb (µg/L)	45 min Desorb (DUP) (µg/L)
93.2	84.7	145.9	96.0
48.0	35.2	33.2	26.5
76.7	81.3	87.0	78.9
4.4	4.4	4.1	4.4
103.6	105.2	140.3	117.5
47.6	43.7	45.8	38.2

Table 37. 2nd Desorption Test Raw Data (5/16/3)

Chemical	RF (AVG)	%RSD	t = 0 (µg/L)	t = 5 (µg/L)
Acetone	0.02	60.0	175.9	150.1
Carbon Disulfide	2.20	34.1	174.0	148.4
Chlorobenzene	2.57	17.5	165.8	132.5
Ethyl Acetate	0.22	20.0	17.4	15.2
Methyl Methacrylate	0.05	17.8	211.6	175.8
Toluene	5.26	18.8	137.4	120.9

Rinse (µg/L)	Rinse (DUP) (µg/L)	45 min Desorb (µg/L)	24 hour Desorb (µg/L)	24 hour Desorb (DUP) (µg/L)
97.2	80.1	72.5	55.7	83.8
53.5	43.3	45.4	29.0	33.2
54.2	52.3	46.7	41.6	49.1
5.7	5.1	4.6	2.3	2.1
71.8	68.9	52.4	43.4	49.4
46.4	41.8	36.3	31.6	35.9

Table 38. SPME 1st Test Raw Data (5/28/3)

Chemical	RF (AVG)	%RSD	Stock Solution (µg/L)	t = 3.5 (µg/L)	t = 5 (µg/L)	t = 7 (µg/L)	t = 9 (µg/L)	t = 11 (µg/L)
Acetone	0.0278	16.4	239.1256203	227.95	253.6	233.13	187.4	147.63
Butyl Alcohol			374.0	471.0	435	248		165
Carbon Disulfide	1.54	30.2	60.7	63.9	67.56	52.49	43.01	35.68
Chlorobenzene	2.3	12.5	114.7	112.8	104.1	89.96	76.08	61.5
Ethyl Acetate	0.20	13.6	43.8	39.4	38.5	35.7	30.25	24.4
Indole			208.0	257.0	180.0	96		70.0
Methyl Methacrylate	0.054	10.1	221.6	204.6	191.1	173.52	149.3	119.3
Toluene	3.81	18.4	69.4	72.5	65.35	58.6	49.94	42.84

Table 39. SPME 2nd Test Raw Data (5/29/3)

Chemical	RF (AVG)	%RSD	Stock Solution (µg/L)	t = 3.5 (µg/L)	t = 5 (µg/L)	t = 7 (µg/L)	t = 9 (µg/L)	t = 11 (µg/L)
Acetone	0.0278	16.4	232.0	251.0	305.7	207.7	166.6	129.2
Butyl Alcohol			458.4	96.0	87.0	46.0	46.0	34.0
Carbon Disulfide	1.54	30.2	106.0	46.3	48.7	27.0	17.4	11.2
Chlorobenzene	2.3	12.5	211.0	148.3	145.0	82.8	50.3	24.6
Ethyl Acetate	0.20	13.6	53.6	28.8	29.0	18.9	13.5	7.9
Indole			107.1	66.0	61.0	0.0	0.0	0.0
Methyl Methacrylate	0.054	10.1	250.3	117.5	113.6	66.8	40.4	204.6
Toluene	3.81	18.4	104.5	87.1	86.8	52.4	32.9	72.5

Table 40. SPME 3rd Test Raw Data (6/7/3)

Chemical	RF (AVG)	%RSD	Stock Solution (µg/L)	t = 3.5 (µg/L)	t = 5 (µg/L)	t = 7 (µg/L)	t = 9 (µg/L)	t = 11 (µg/L)
Acetone	0.0278	16.4	198.0	178.8	158.0	122.4		
Butyl Alcohol			0.270	0.472	0.353	0.333	0.280	0.341
Carbon Disulfide	1.54	30.2	92.4	61.7	56.9	50.3		
Chlorobenzene	2.3	12.5	160.2	133.8	131.1	110.6		
Ethyl Acetate	0.20	13.6	35.4	32.1	31.2	26.6		
Indole			0.210	0.290	0.215	0.207	0.107	0.189
Methyl Methacrylate	0.054	10.1	120.7	111.8	112.3	90.7		
Toluene	3.81	18.4	65.3	51.3	50.4	44.0		

Table 41. SPME 4th Test Raw Data (6/14/3)

Chemical	Stock Solution (µg/L)	t = 3.5 (µg/L)	t = 5 (µg/L)	Port 1 (µg/L)	Port 2 (µg/L)
Butyl Alcohol	589.0	752.0	765.0	661.0	43.0
Indole	3009.0	2117.0	2063.0	2343.0	75.0
*Port 1 is before the reactor		*Port 2 is after the reactor			

Table 42. SPME 5th Test Raw Data (6/15/3)

Chemical	Stock Solution (µg/L)	t = 3.5 (µg/L)	t = 5 (µg/L)	Port 1 (µg/L)	Port 2 (µg/L)
Butyl Alcohol	374.0	344.0	311.0	491.0	32.0
Indole	2005.0	1798.0	1987.0	2029.0	49.0
*Port 1 is before the reactor		*Port 2 is after the reactor			

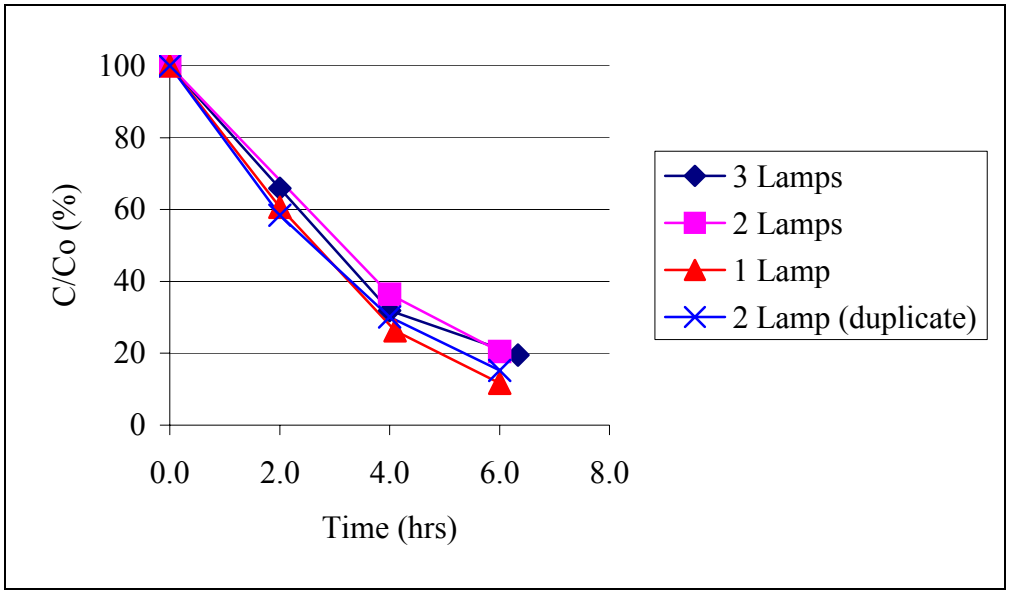

Figure 30. Normalized removal of toluene over the course of 6 hours. The flow rate in all of the experiments was 10 mL/min and the system was operated in circulation mode with a 1-liter source tank. Removal represents overall removal in the system.

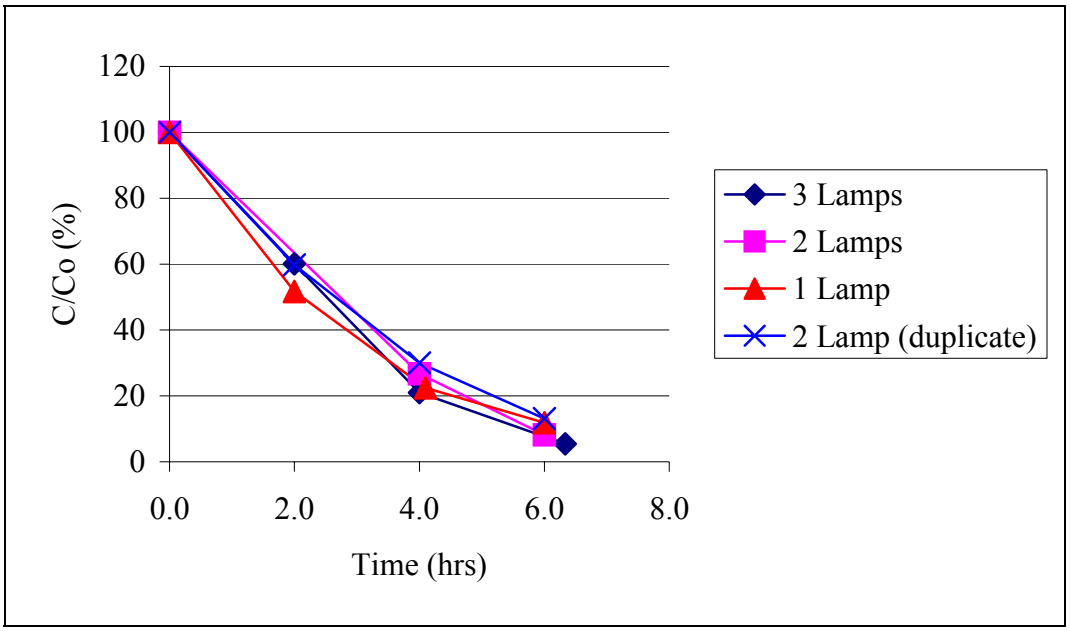

Figure 31. Normalized removal of methyl methacrylate over the course of 6 hours. The flow rate in all of the experiments was 10 mL/min and the system was operated in circulation mode with a 1-liter source tank. Removal represents overall removal in the system.

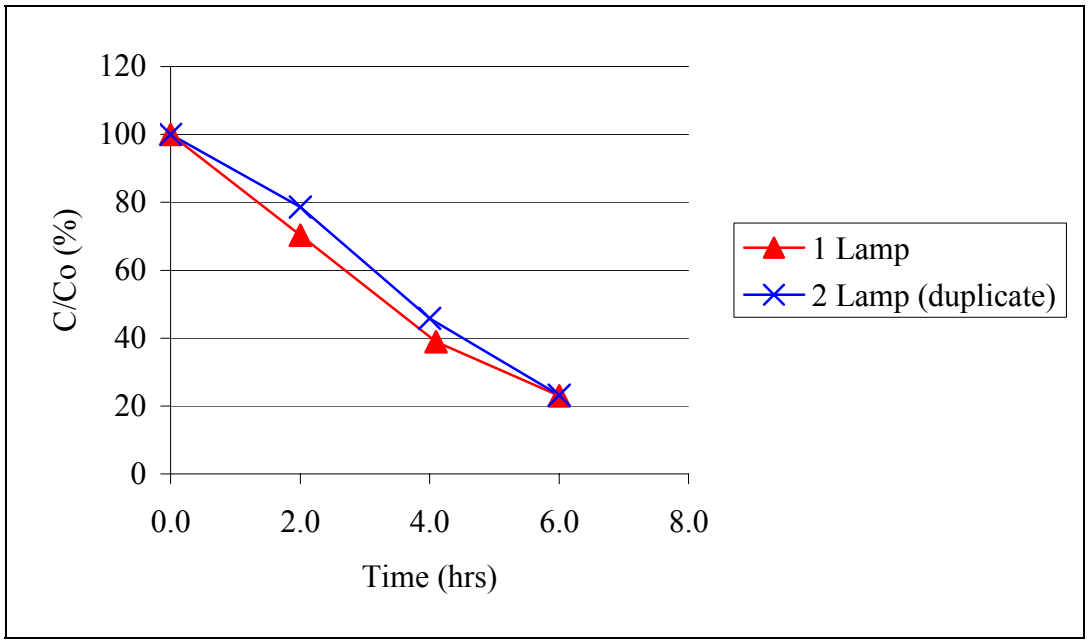

Figure 32. Normalized removal of carbon disulfide over the course of 6 hours. The flow rate in all of the experiments was 10 mL/min and the system was operated in circulation mode with a 1-liter source tank. Removal represents overall removal in the system.

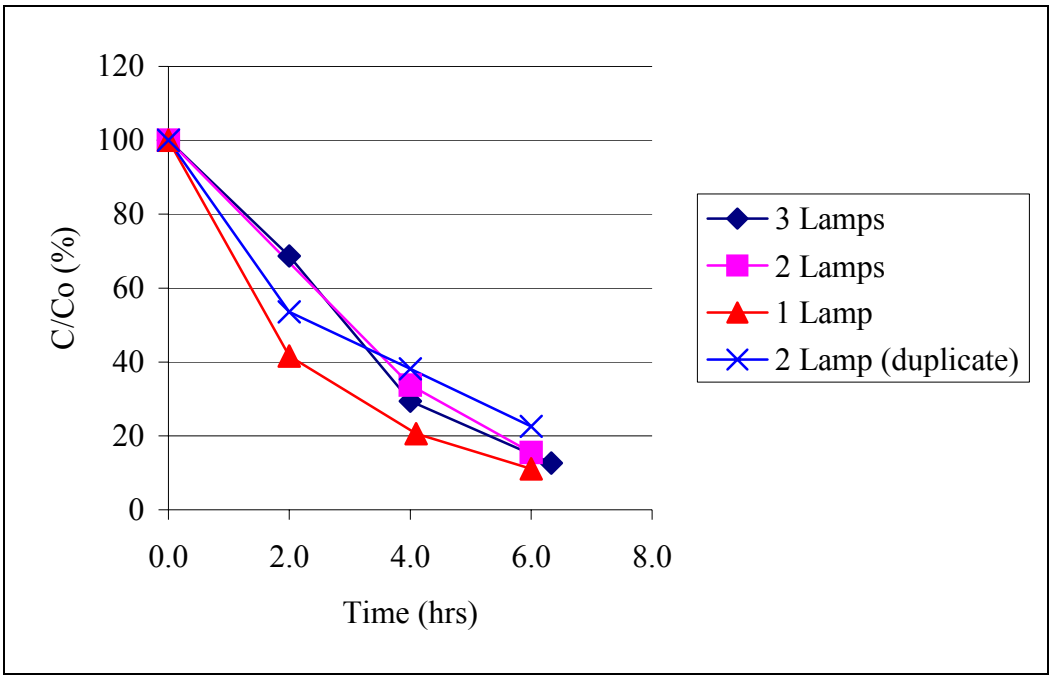

Figure 33. Normalized removal of ethyl acetate over the course of 6 hours. The flow rate in all of the experiments was 10 mL/min and the system was operated in circulation mode with a 1-liter source tank. Removal represents overall removal in the system.

REFERENCES

Anheden, M.; Goswami, D. Y.; Svedberg, G., 1996. Photocatalytic Treatment of Wastewater From 5-Fluorouracil Manufacturing. *Transactions of the ASME*, 118:2.

Bekbölet, M.; Baleioglu, I., 1996. Photocatalytic Degradation Kinetics of Humic Acid in Aqueous TiO_2 Dispersions: The Influence of Hydrogen Peroxide and Bicarbonate Ion. *Wat. Sci. Tech.*, 34:9:73.

Bideau, M.; Claudel, B.; Dubien, C.; Faure, L.; Kazouan, H., 1995. On the Immobilization of Titanium-Dioxide in the Photocatalytic Oxidation of Spent Waters. *Journal of Photochemistry and Photobiology A-Chemistry*, 91:2:137.

Blake, D. M., 1999. Bibliography of Work on the Heterogeneous Photocatalytic Removal of Hazardous Compounds from Water and Air. *National Renewable Energy Laboratory*, August 1999.

Blake, D. M.; Webb, J.; Turchi, C.; Magrini, K., 1991. Kinetic and Mechanistic Overview of TiO_2-Photocatalyzed Oxidation Reactions in Aqueous-Solution. *Solar Energy Materials*, 24:584.

Block, S. S.; Seng, V. P.; Goswami, D. W., 1997. Chemically Enhanced Sunlight for Killing Bacteria. *Journal of Solar Energy Engineering*, 119:85.

Bonsen, E.; Schroeter, S.; Jacobs, H.; Broekaert, J. A. C., 1997. Photocatalytic Degradation of Ammonia with TiO_2 as Photocatalyst in the Laboratory and under the use of Solar Radiation. *Chemosphere*, 34:7:1431.

Butterfield, I. M.; Christensen, P. A.; Curtis, T. P.; Gunlazuardi, J., 1997. Water Disinfection Using an Immobilised Titanium Dioxide Film in a Photochemical Reactor with Electric Field Enhancement. *Wat. Res.*, 31:3:675.

Chen, P. H.; Chen, C.; Jenq, C. H., 1995. TiO_2 Photocatalysis to Remove the Trace Organic in Drinking Water. *Water Supply*, 13:3/4:29.

Cooper, A. T.; Goswami, Y. D.; Block, S. S., 1998. Solar Photochemical Detoxification and Disinfection for Water Treatment in Tropical Developing Countries. *J. Adv. Oxid. Technol.*, 3:2:151.

Cooper, A. T.; Goswami, Y. D., 1999. Evaluation of Solar Photosensitization of Benzene, Toluene, and *Escherichia Coli* with Methylene Blue and Rose Bengal. Proceedings of the Renewable and Advanced Energy Systems for the 21st Century in Lahaina, Maui, HA, 1.

Crittenden, J. C.; Liu, J.; Hand, D. W.; Perram, D. L., 1997. Photocatalytic Oxidation of Chlorinated Hydrocarbons in Water. *Wat. Res.*, 31:3:429.

Davis, A.P.; Hao, O. J., 1991. Reactor Dynamics in the Evaluation of Photocatalytic Oxidation Kinetics. *Journal of Catalysis*, 131:285.

Denisov, E. T., 1977. *Liquid-Phase Oxidation of Oxygen-Containing Compounds*. Consultants Bureau, New York.

D'Oliveira, J.; Al-Sayyed, G.; Pichat, P., 1990. Photodegradation of 2- and 3-Chlorophenol in TiO_2 Aqueous Suspensions. *Environ. Sci. Technol.*, 24:7:990.

Emanuel, N. M., 1984. *Oxidation of Organic Compounds: Medium Effects in Radical Reactions*. Permagon Press, Oxford.

The Federal Register, Washington, 36:236:68088.

Gao, X.; Wachs, I., 1999. Titania-Silica as Catalysts: Molecular Structural Characteristics and Physico-Chemical Properties. *Catalysis Today*, 51:233.

Glaze, W. H., 1990. Chemical Oxidation. Chapter 12, *Water Quality and Treatment: A Handbook of Community Water Supplies*, Pontius, F. W., AWWA, 4:747.

Goswami, D. Y.; Mathur, G. D.; Jotshi, C. K., 1994. Methodology of Design of Non-Concentrating Solar Detoxification Systems. *Engineering Systems Design and Analysis*, 3:1.

Goswami, Y.D., 1995. Engineering of Solar Photocatalytic Detoxification and Disinfection Processes. Chapter 3, *Advances in Solar Energy*, Boer, K. W., ASES, 10:165.

Goswami, Y. D.; Blake, D. M., 1996. Cleaning up with Sunshine. *Mechanical Engineering*, August 1996:56.

Goswami, D. Y.; Trivedi, D. M.; Block S. S., 1997. Photocatalytic Disinfection of Indoor Air. *Journal of Solar Energy Engineering*, 119: 92.

Goswami, Y. D., 1999. Recent Developments in Photocatalytic Detoxification and Disinfection of Water and Air. Proceedings of the ISES 1999 Solar World Congress in Jerusalem, Israel.

Hand, D. W.; Perram, D. L.; Crittenden, J. C., 1995. Destruction of DBP Precursors with Catalytic Oxidation. *Journal AWWA*, June 1995:84.

Hingorani, S.; Greist, H.; Goswami, T.; Goswami, Y., 2000. Clean-up of Contaminated Indoor Air Using Photocatalytic Technology. Proceedings of the 12th Symposium on Improving Building Systems in Hot and Humid Climates in San Antonio, TX.

Brendl, Andreas; Beck, Bernd; Clark, Timothy; Glen, Robert. "Prediction of the n-Octanol/Water Partition Coefficient, logP, Using a Combination of Semiempirical MO-Calculations and a Neural Network." Computer Chemistry Center. January 16, 2003. June 18, 2003 <http://www.ccc.uni-erlangen.de/jmolmod/sample/70030142.htm>

Eaton Chemical Incorporated. "Eaton Chemical Incorporated: Solvent List." July 15, 2001. June 18, 2003 <http://www.echeminc.com/Solvents.htm>.

US Environmental Protection Agency. "Technology Transfers Network Air Toxics Website: Methyl Methacrylate." February 12, 2003. June 18, 2003 <http://www.epa.gov/ttnatw01/hlthef/methylme.html>.

General Electric Company. "Fused Quartz Properties and Usage Guide." October 11, 2000. June 18, 2003 <http://www.quartz.com/gedata.html>.

Degussa AG. "Aerosil." June 25, 2003 <http://x:x@www2.sivento.de/sivento/silica/html/e/solutions_products/datasheet/silica_datasheet.asp?id=625&definition=2>.

Kawaguchi, H.; Furuya, M., 1990. Photodegradation of Monochlorobenzene in Titanium Dioxide Aqueous Suspensions. *Chemosphere*, 21:12:1435.

Klausner, J. F.; Goswami, D. Y., 1993. Solar Detoxification of Wastewater Using Nonconcentrating Reactors. *AIChE Symposium Series*, 295:89:445.

Klausner, J. F.; Martin, A. R.; Goswami, D. Y., 1994. On the Accurate Determination of Reaction Rate Constants in Batch-Type Solar Photocatalytic Oxidation Facilities. *Journal of Solar Energy Engineering*, 116:19.

Lane, H. W.; Behrend, A. F., 1999. Advanced Life Support Plan. Document #CTSD-ADV-348 (REV B) presented for the Crew and Thermal Systems Division in Houston, TX.

Lange, K. E.; Lin, C. H., 1998. Advanced Life Support Program: Requirements Definition and Design Considerations. Document # CTSD-ADV-245 (REV A) presented for the Crew and Thermal Systems Division in Houston, TX.

Lichtin, N. N.; Dong, J.; Vijayakumar, K. M., 1992. Photopromoted TiO_2-Catalyzed Oxidative Decomposition of Organic Pollutants in Water and in the Vapor Phase. *Water Poll. Res. J. Canada*, 27:1:203.

Liu, T.; Cheng, T. 1995. Effects of SiO_2 on the Catalytic Properties of TiO_2 for the Incineration of Chloroform. *Catalysis Today*, 26:71.

Londeree, D. J., 2002. Silica-titania Composites for Water Treatment. Thesis presented to the graduate school of the University of Florida.

Luo, Yang,; Ollis, D. F., 1996. Heterogeneous Photocatalytic Oxidation of Trichloroethylene and Toluene Mixture in Air: Kinetic Promotion and Inhibition, Time-Dependent Catalysis Activity. *Journal of Catalysis*, 163:1.

Matsuda, A.; Kotani, Y.; Kogure, T.; Tatsumisago, M.; Minami, T., 2000. Transparent Anatase Nanocomposite Films by the Sol-Gel Process at Low Temperatures. *J. Am. Ceram. Soc.*, 83:1:229.

Matthews, R. W., 1987. Photooxidation of Organic Impurities in Water Using Thin Films of Titanium Dioxide. *Journal of Physical Chemistry*, 91:3328.

Matthews, R. W., 1993. Photocatalysis in Water Purification: Possibilities, Problems, and Prospects. *Photocatalytic Purification and Treatment of Water and Air*, Ollis, D. F.; Al-Ekabi, H., Proceedings of the 1st International Conference on TiO_2 Photocatalytic Purification and Treatment of Water and Air in London, Ontario, and Canada, 121.

Nawrocki, J., 1997. The Silanol Group and its Role in Liquid Chromatography. *Journal of Chromatography A*, 779:29.

Nishida, K.; Ohgaki, S., 1994. Photolysis of Aromatic Chemical Compounds in Aqueous TiO_2 Suspensions. *Wat. Sci. Tech.*, 30:9:39.

Ollis, D. F., 1985. Contaminant Degradation in Water. *Environmental Science and Technology*, 19:480.

Ollis, D. F.; Pelizzetti, E.; Serpone, N., 1991. Destruction of Water Contaminants. *Environ. Sci. Technol.*, 25:9:1523.

Ollis, D.F.; Al-Ekabi, H., 1993. *Photocatalytic Purification and Treatment of Water and Air*. Proceedings of the 1st International Conference on TiO_2 Photocatalytic Purification and Treatment of Water and Air in London, Ontario, and Canada.

Rohrbacher, J., 2001. Photocatalytic Oxidation of Chlorobenzene Using Titania Catalyst. Non-Thesis project presented to the graduate school of the University of Florida.

Sakthivel, S.; Geissen S. U.; Bahnemann, D. W.; Murugesan, V.; Vogelpohl, A., 2002. Enhancement of Photocatalytic Activity by Semiconductor Heterojunctions: Alpha-Fe_2O_3, WO_3, and CdS Deposited on ZnO. *Journal of Photochemistry and Photobiology A-Chemistry*, 148:283.

Schwarzenbach, René P., 1993. *Environmental Organic Chemistry*, John Wiley and Sons, New York.

Serpone, N., 1995. Brief Introductory Remarks on Heterogeneous Photocatalysis. *Solar Energy Materials and Solar Cells*, 38:369.

Srinivasan, M.; Klausner, J. F.; Jotshi, C. K.; Goswami, D. Y., 1997. Solar Photocatalytic Treatment of BTEX Contaminated Groundwater. Proceedings of the ISES 1997 Solar World Congress.

Standard Methods for the Examination of Water and Wastewater, 1998 (20th ed.). APHA, AWWA, and WEF, Washington.

Torimoto, T.; Ito, S.; Kuwabata, S.; Yoneyama, H., 1996. Effects of Adsorbents Used as Supports for Titanium Dioxide Loading on Photocatalytic Degradation of Propyzamide. *Environmental Science & Technology*, 30:4:1275.

Turchi, C. S.; Ollis, D. F., 1989. Mixed Reactant Photocatalysis: Intermediates and Mutual Rate Inhibition. *Journal of Photocatalysis*, 119:483.

Turchi, C. S.; Ollis, D. F., 1990. Photocatalytic Degradation of Organic-Water Contaminants-Mechanisms Involving Hydroxyl Radical Attack. *Journal of Catalysis*, 122:178.

USEPA, 1992. Methods for the Determination of Organic Compounds in Drinking Water. EPA/600/R-92/129, Springfield.

Verschuerren, K., 1983. *Handbook of Environmental Data on Organic Chemicals* (2nd Edition). Van Nostrand Reinhold Company, New York.

Vidal, A., 1998. Developments in Solar Photocatalysis for Water Purification. *Chemosphere*, 36:12:2593.

Vijayaraghavan, S., 2000. The Effect of pH, UV Intensity, and Dissolved Oxygen Content on the Photocatalytic Destruction of Toluene in Water. Thesis presented to the graduate school of the University of Florida.

Windholz, M., 1976. *The Merck Index: An Encyclopedia of Chemicals and Drugs* (9th Edition). Merck & Co., Inc., Rahway, NJ.

Yaws, C. L., 1999. *Chemical Properties Handbook: Physical, Thermodynamic, Environmental, Transport, Safety, and Health Related Properties for Organic and Inorganic Chemicals*, McGraw-Hill Company, New York.

Yu, H.; Wang, S., 2000. Effects of Water Content and pH on Gel-Derived TiO_2-SiO_2. *Journal of Non-Crystalline Solids*, 261:260.

Zaidi, A. H.; Goswami, D. Y., 1995. Solar Photocatalytic Post-Treatment of Anaerobically Digested Distillery Effluent. Proceedings of the American Solar Energy Society Annual Conference in Minneapolis, MN., 51.

BIOGRAPHICAL SKETCH

Frederick Roland Holmes was born in Bradenton, Florida, on April 13, 1979. He is the first son born to his parents Stanley and Patricia Holmes. He has one younger brother Vincent and a younger sister Shannon. Frederick grew up in the city of Spring Hill, Florida, where he graduated from high school in June of 1997. During his junior year at Springstead High School he became involved in the Envirothon competition, which became the inspiration for his future occupation as an environmental engineer.

After high school, Frederick moved to Gainesville where he attended the University of Florida to obtain his Bachelor of Science in Environmental Engineering degree. During his undergraduate work he met his wife April through work with the dorm area government. The two were married in July of 2002.

Frederick entered graduate school in the spring semester of 2002. Under the guidance of his advising professor, Dr. Paul A. Chadik, Frederick performed research on the use of photocatalysis as a finishing process for NASA. The results of that research are found in the preceding thesis.